Mastozoología Neotropical
ISSN: 0327-9383
ISSN: 1666-0536
kittlein@gmail.com
Sociedad Argentina para el Estudio de los Mamíferos
Argentina

Brito, Jorge; Tinoco, Nicolás; Burneo, Santiago; Koch, Claudia; Arguero, Alfonso; Vargas, Rocío; Pinto, Miguel
A NEW SPECIES OF SPINY MOUSE, GENUS *Neacomys* (CRICETIDAE: SIGMODONTINAE) FROM CORDILLERA DEL CÓNDOR, ECUADOR
Mastozoología Neotropical, vol. 28, núm. 1, 2021, Enero-Junio, p. 507
Sociedad Argentina para el Estudio de los Mamíferos
Tucumán, Argentina

Mastozoología Neotropical, 28(1), Mendoza, 2021
Versión on-line ISSN 1666-0536
https://doi.org/10.31687/saremMN.21.28.1.0.23

Sección Especial
EL ÚLTIMO NATURALISTA TIPÓLOGO:
CONTRIBUCIONES EN HONOR A ELIO MASSOIA (1936-2001)
Editores: Ulyses F. J. Pardiñas y Carlos Galliari
Artículo

A NEW SPECIES OF SPINY MOUSE, GENUS *Neacomys* (CRICETIDAE: SIGMODONTINAE) FROM CORDILLERA DEL CÓNDOR, ECUADOR

Jorge Brito[1], Nicolás Tinoco[2], Santiago Burneo[2], Claudia Koch[3], Alfonso Arguero[4], Rocío Vargas[1] and C. Miguel Pinto[5]

[1]Instituto Nacional de Biodiversidad (INABIO), Pasaje Rumipamba 341 y Av. de los Shyris, PB 17-07-8976, Quito, Ecuador. [Correspondence: Jorge Brito <jorgeyakuma@yahoo.es>]
[2]Sección de Mastozoología, Museo de Zoología, Facultad de Ciencias Exactas y Naturales, Pontificia Universidad Católica del Ecuador, Quito, Pichincha, Ecuador, Quito, Ecuador.
[3]Zoologisches Forschungsmuseum Alexander Koenig (ZFMK), Bonn, Germany.
[4]Departamento de Biología, Facultad de Ciencias, Escuela Politécnica Nacional, Quito, Ecuador.
[5]Observatorio de Biodiversidad Ambiente y Salud (OBBAS), Quito, Ecuador.

ABSTRACT. We describe a new species within the sigmodontine rodent genus *Neacomys* that inhabits the Cordillera del Cóndor, southeastern Ecuador. The new *Neacomys* is easily distinguished from other species in the genus by the combination of the following characters: small size (∼69 mm of head-body length), moderately long tail (∼55.5% longer than head-body length), venter fur with golden color, very large postglenoid foramen, anterocone of upper first molar undivided, presence of paralophule and spur of enamel on the upper first molar, upper molars with small labial cusps, and lower molars with small lingual cusps. Phylogenetic analyses based on cytochrome b gene (Cyt b) sequences indicate that the new species is sister to the "*tenuipes*" and "*dubosti*" groups. Given distinctive morphological characters we propose the recognition of a new species group for this new species. This new *Neacomys*, endemic to the Cordillera del Cóndor, presents a genetic distance between 12% and 15% to other species. Finally, we consider that *N. amoenus carceleni* exhibits sufficient distinctive genetic and morphological characteristics to be considered as a species. With the new entity described here and the change of status of *N. carceleni*, the diversity of the genus rises to 17 species. In this context, this small terrestrial oryzomyine appears an ideal candidate to contribute relevant information to the complex puzzle of Amazonian landscape evolution.

RESUMEN. Una nueva especie de ratón espinoso del género *Neacomys* (Cricetidae: Sigmodontinae) de Cordillera del Cóndor, Ecuador. Describimos una nueva especie de roedor sigmodontino del género *Neacomys* que habita en la cordillera del Cóndor, sureste de Ecuador. La nueva entidad se distingue fácilmente de sus congéneres por la combinación de los siguientes caracteres: tamaño pequeño (longitud cabeza-cuerpo ∼69 mm), cola larga (∼55.5 % más que la longitud cabeza-cuerpo), vientre con pelaje dorado; foramen postglenoideo muy grande, anterocono del primer molar superior no dividido, presencia de paralófulo y una proyección de esmalte en el primer molar superior; molares superiores con cúspides labiales reducidas y molares inferiores con cúspides linguales reducidas. Los análisis filogenéticos usando el gen mitocondrial citocromo b (Cyt b) indican que la especie nueva es hermana a los grupos "*tenuipes*" y "*dubosti*". Al presentar caracteres morfológicos distintivos, proponemos el reconocimiento de un nuevo grupo para contenerla. Esta nueva especie, endémica de la Cordillera del Cóndor, presenta una distancia genética entre 12 % y 15 % con los

Recibido: 12 septiembre 2020. Aceptado: 14 febrero 2021. Editor asociado: U. F. J. Pardiñas & C. A. Galliari.

grupos ya conocidos. Finalmente, consideramos que *N. amoenus carceleni* presenta características morfológicas y genéticas suficientemente diferentes para ser tratada como especie válida. Con la nueva entidad aquí descrita y el cambio de categoría de *N. carceleni*, la diversidad del género *Neacomys* asciende a 17 especies. En este contexto, este pequeño orizomino terrestre parece ser un candidato ideal para contribuir información relevante al complejo rompecabezas del panorama evolutivo amazónico.

Palabras clave: Amazonia, Andes, diversidad, montañas extra-andinas, Oryzomyini.
Key words: Amazonia, Andes, diversity, extra-Andean mountains, Oryzomyini.

INTRODUCTION

The genus *Neacomys* Thomas, 1900, distributed from Panama to Bolivia, inhabits lowland forests of southernmost Central America and Amazonia, and lower Andean forests (Weksler & Bonvicino 2015; Hurtado & Pacheco 2017; Pardiñas et al. 2017; Sánchez-Vendizú et al. 2018; Semedo et al. 2020). These are oryzomyine rodents of small size (head-body length of 62-105 mm), with short and grooved spines and regular guard hair, a reddish-brown dorsal coloration and marked belly countershaded. Females have eight mammae in inguinal, abdominal, postaxial and pectoral pairs. The skulls share evident supraorbital crests, small and pentalophodont molars, mesoloph developed in the two first upper molars fused to the mesostyle, and lacks accessory roots (Voss et al. 2001).

Neacomys includes 17 species of terrestrial rodents (Weksler & Bonvicino 2015; Hurtado & Pacheco 2017; Pardiñas et al. 2017; Sánchez-Vendizú et al. 2018; Semedo et al. 2020), assigned to four species groups with molecular and morphological agreement (Hurtado & Pacheco 2017; Sánchez-Vendizú et al. 2018; Semedo et al. 2020): "*dubosti*", "*paracou*", "*spinosus*", and "*tenuipes*". Part of this diversity has recently been described (Hurtado & Pacheco 2017; Sánchez-Vendizú et al. 2018; Semedo et al. 2020), indicating an active process of revision of this oryzomyine.

Based on material collected in the Cordillera del Cóndor, an isolated mountain ridge in southeastern Ecuador, we describe a new species of *Neacomys*. This elevated terrain, a branch of the Andes with biogeographical links to the Guiana shield (Berry et al. 1995), is a hotspot of species richness and endemism of plants (Schulenberg & Awbrey 1997) and animals (Guayasamin & Bonaccorso 2011; Freile et al. 2014; Almendáriz et al. 2014; Reyes-Puig et al. 2017). Likewise, based on material from different localities in the Amazon of Ecuador, we reviewed the taxonomic status of *Neacomys amoenus carceleni* (Hershkovitz, 1940).

MATERIALS AND METHODS

Studied specimens

We conducted collecting expeditions in five localities of the Cordillera del Cóndor, during assessments of environmental impact developed between the years 2010-2016. For the capture of terrestrial small mammals, we used Sherman live traps (7.5 × 9 × 27 cm; H. B. Sherman Traps, Tallahassee, Florida) and pitfall traps (Voss et al. 2001) and followed animal management guidelines recommended by Sikes et al. (2016). We trapped for three consecutive days in each study site, employing a variable number of traps. The sampling effort averaged 2 000 trap/nights, and all specimens belonging to *Neacomys* were captured in pitfall traps. These individuals and other *Neacomys* were directly compared to numerous oryzomyines deposited in Ecuadorian and Colombian mammal collections, according to the following detail: Museo de la Escuela Politécnica Nacional (MEPN; Quito, Ecuador); Museo de Zoología de la Pontificia Universidad Católica del Ecuador (QCAZ; Quito, Ecuador); Instituto de Investigación de Recursos Biológicos Alexander von Humboldt (IAvH-M, Bogotá, Colombia), and Instituto Nacional de Biodiversidad (MECN; formerly known as Museo Ecuatoriano de Ciencias Naturales; Quito, Ecuador). All the studied material is listed in APPENDIX 1 and **Table** S1.

DNA Extraction, amplification, and sequencing

We obtained sequences of the mitochondrial cytochrome *b* gene (Cyt b) from Ecuadorian *Neacomys amoenus carceleni*, *N. rosalindae*, *N. tenuipes*, and the new species here described from Cordillera del Cóndor (*Neacomys* sp. nov.). We conducted PCR amplifications with the primers MVZ05, MVZ14 and MVZ16H (Smith & Patto 1993), with the following amplification profile: an initial denaturation at 94°C for 180 s, 35 cycles of denaturation at 94°C for 45 s, primer annealing at 45°C for 30 s, and the final elongation at 72°C for 600 s (Hurtado & Pacheco 2017). In some cases, the annealing temperature was modified to 47°C for 60 s. For difficult samples we used the primer pair L-14115 and H-14963 (Sullivan et al. 2000) with the following amplification profile: initial denaturation at 94°C for 120 s, 35 cycles of denaturation at 94°C for 60 s, primer annealing at 48°C for 60 s, elongation at 72°C for 60 s, and final elongation at 72°C for 600 s. The PCR products were sequenced by Macrogen Inc., South Korea. The sequences were deposited in GenBank; accession numbers are provided in **Table** S2.

Phylogenetic analyses

The sequences were edited and assembled using the Geneious R11 program (<https://www.geneious.com>) and aligned using the Clustal-W tool. We used the program PartitionFinder2 (Lanfear et al. 2017) to obtain the best partition and scheme of substitution models; the alignment was divided in three partitions with the following models: SYM+I+, HKY+I+G, GTR+I+G for first, second and third codon positions of the CYTB gene and implemented in the Bayesian analysis. We conducted analyses of Maximum Likelihood (ML) and Bayesian Inference (BI). The ML analysis was conducted with RAxML 8.2.10 (Stamatakis 2014) under the GTRGAMMA model, with 10 alternative runs on randomized maximum parsimony starting trees. Nodal support (BS) was assessed with the rapid bootstrapping algorithm under the MRE-based Bootstopping criterion (1 000 replicates). The BI analysis was conducted with MrBayes 3.2 (Ronquist et al. 2012); four chains were run for 10 000 000 generations, with a sampling every 1 000 generations and a burn-in of 0.25. Convergence was evaluated by the effective sample size (EES) and the potential scale reduction factor (PSRF). For most of the parameters the EES should be $\geq$200 and for the PSRF most of the values of the parameters should be between 1.0 and 1.2. In both analyzes we used the same species from Hurtado & Pacheco (2017), Sánchez-Vendizú et al. (2018), and Semedo et al. (2020) as out-groups. We calculate the uncorrected genetic distances (p-distance) in MEGA X (Kumar et al. 2018). We obtained the distance between each of the species, and the genetic variation within each species. Additionally, we perform a grouping of the sequences to obtain the genetic distance between the groups.

Micro CT Scanning

For a more detailed recording of the morphological characters of the skull, the holotype of the new species described here (MEPN 12081; see below) was scanned using a high-resolution micro-computed tomography (micro-CT) desktop device (Bruker SkyScan 1272, Kontich, Belgium) at the Zoologisches Forschungsmuseum Alexander Koenig (ZFMK, Bonn, Germany). To avoid movements during scanning the skull was placed in a small plastic container embedded in cotton wool. Acquisition parameters resulted in a scan duration of 1 h 33 min and comprised: 2 connected scans with 627 projections; 0.3° rotation steps over 180°; spatial resolution of 13.005786 μm; 35 kV; 200 μA; no filter; frame averaging of 7; random movement of 15; 800 ms exposure time. The CT-dataset was reconstructed with N-Recon software version 1.7.1.6 (Bruker MicroCT, Kontich, Belgium) and rendered in three dimensions using CTVox for Windows 64 bits version 3.0.0 r1114 (Bruker MicroCT, Kontich, Belgium). The reconstructed image stacks of the CT-scan were uploaded to www.morphdbase.de, and can be accessed via the direct links <http://www.morphdbase.de/?C_Koch_20200908-S-8.1> (for the cranium) and <www.morphdbase.de/?C_Koch_20200908-S-7.1> (for the mandible).

Anatomy and measurements

We follow the terminology of external and cranial characters of Reig (1977), Carleton & Musser (1989)), Patton et al. (2000), Voss et al. (2001), and Hurtado & Pacheco (2017). The soft anatomy was characterized based on the concepts of Carleton (1973), Vorontsov (1967), and Pardiñas et al. (2020). We followed the terminology and definitions employed by Tribe (1996) and Costa et al. (2011) for age classes and restricted the term "adults" for those in categories 3 and 4. We obtained the following external measurements, some of them registered in the field and others recorded from tags: head and body length (HB), tail length (TL), hind foot length (HF, including claw), ear length (E), longest mystacial vibrissae (LMV), length of longest superciliary vibrissae (LSV), length of longest genal vibrissae (LGV), and body mass (W, in grams). Cranial measurements (we follow Carleton & Musser 1989; Patton et al. 2000; Voss et al. 2001; Hurtado & Pacheco 2017) were obtained with a digital caliper at a precision of 0.01 mm: condylo-incisive length (CIL), zygomatic breadth (ZB), breadth of braincase (BB), least interorbital breastema (DL), crown length of maxillary toothrow (MTRL); length of incisive foramen (IFL), length of palatal bridge (PBL), mastoid breadth (MB), length of basioccipital (BOL), breadth of foramen mesopterygoid (MPFW), breadth of zygomatic plate (ZPB), cranial depth (CP), and length of mandible (LM).

Morphometric analyses

The dataset analyzed comprises 16 craniodental measurements, from 144 specimens belonging to five taxa: *Neacomys amoenus amoenus* (n=50), *N. amoenus carceleni* (n=19), *N. rosalindae* (n=48), *N. spinosus* (n=12), and *Neacomys* sp. nov. (n=15) (**Table** S1). We selected *N. amoenus amoenus*, *N. rosalindae* and *N. spinosus* to compare with *N. amoenus carceleni* and *Neacomys.* sp. nov. because their geographical distributions are close (i.e., *N. spinosus*), overlap (i.e, *N. rosalindae*), and because of their current conspecific status (i.e., *N. amoenus amoenus*). Each measurement was tested for normality using the Shapiro-Wilk test. Seven of these measurements were not normally distributed, thus the whole dataset was log-transformed to improve its statistical properties. The dataset contained 5% of missing data. Therefore, to avoid eliminating individuals or measurements from the analyses, we performed imputation of missing data. Among the several options to impute missing data, we choose the expectation-maximization (EM) method because of its higher accuracy (Strauss et al. 2003; Clavel et al. 2014). We generated 100 imputed datasets (m=100), which we averaged to obtain a single imputed dataset. Prior to these analyses we checked for unusually high pair-wise correlations among measurements. No pair of variables had a correlation coefficient > 0.95, so no variables were eliminated. We conducted 6 multivariate analyses, 3 principal component analyses (PCA) and 3 discriminant function analyses (DFA) using the following 3 combinations of taxa: i) *Neacomys* sp. nov., *N. amoenus carceleni*, and *N. amoenus amoenus,* ii) *Neacomys* sp. nov., *N. amoenus carceleni*, and *N. spinosus*, and iii) *Neacomys* sp. nov., *N. amoenus carceleni*, and *N. rosalindae*. All analyses were performed in R version 3.6.2 (R Core Team 2019). Imputation of missing data was conducted with the Amelia II package, version 1.7.6 (Honaker et al. 2011), and the univariate and multivariate analyses were performed with the R script MorphoTools version 1.1 (Koutecký´ 2015).

Table 1
Genetic p-distances in percentages (%) between groups of species recognized within the genus *Neacomys*.

Groups		1	2	3	4	5
1	*spinosus*					
2	*tenuipes*	8.60				
3	*paracou*	11.85	9.89			
4	*dubosti*	7.75	6.02	10.75		
5	*auriventer* sp. nov.	10.32	9.21	13.15	9.55	

Operational criteria for delimiting species

Species delimitation was performed following the unified species concept (De Queiroz 2005, 2007). This concept is flexible because its only requisite to define a species is that it is "a separately evolving lineage segment" (De Queiroz 2007). The secondary defining properties of a species (e.g., monophyly and diagnosability) serve as lines of evidence or operational criteria for delimiting species (De Queiroz 2007). In this work, our lines of evidence for delimiting species are morphological and molecular data. The morphological diagnosability was based on discrete internal and external morphological characters, and continuous morphometric measurements. The molecular diagnosability was based on genetic distances considered standard for differentiating mammal species (i.e., Bradley & Baker 2001), and the recovery of reciprocally monophyletic groups.

RESULTS

Phylogenetic analyses

The ML and BI analyzes recovered the monophyly of the genus *Neacomys* (**Fig**. 1) and produced similar topologies in most cases, although in some species (*N. marajoara*, *N. musseri*, *N. vossi*, *N. xingu* and one sample of *N. amoenus*) there were certain differences at the interspecific level. It is possible to identify four main clades that correspond to the groups: "*paracou*" (bootstrap support [BS]=100, posterior probability [PP]=1.00), "*spinosus*" (BS=100, PP=1.00), "*dubosti*" (BS=68 , PP=0.84), "*tenuipes*" (BS=62, PP=0.98); in addition, the samples from the Cordillera del Cóndor integrate a monophyletic clade (BS=100; PP=1.00) related to the "*dubosti* + *tenuipes*" groups (**Fig**. 1). The levels of genetic differentiation among these groups are between 9.21% to 13.15% (**Table** 1). The specimens from the Cordillera del Cóndor present a genetic divergence of 11.80% to 14.94% (**Table** 2) with respect to the other species.

Within the "*spinosus*" group (**Fig**. 2), *N. vargasllosai* (BS=97, PP=1.00) and *N. spinosus* (BS=100, PP=1.00) formed strongly supported clades. The clade of *N. amoenus* sensu lato (BS=87, PP=0.99) presented two main clades: *N. a. carceleni* (BS=50, PP=0.8) and *N. amoenus* "Northern Peru [NP]/Central Andean-Amazonian [CCA]/Brazil-Bolivia [BB]" (BS=-, PP=1.00). Within the latter clade three monophyletic subclades were identified: Northern Peru-NP (BS=56, PP=0.88), the Central Andes and Amazon of Peru and Brazil-CCA (BS=70, PP=-) and Northern Mato Grosso in Brazil and the Northeast of Santa Cruz in Bolivia-BB (BS=87, PP=1.00). The level of genetic differentiation between the clade of *N. a. carceleni* and *N. a. amoenus* NP/CCA/BB was 3.26% (**Table** 2), while the genetic distances between the three subclades of *N. amoenus* (NP/CCA/BB) were between 1.94% and 2.71% (**Fig**. S1).

Taxonomic comparisons: Cordillera del Cóndor population is distinguished from other *Neacomys* groups based on tail length, which is ∼55% longer than head-body length, while it is short in the "*tenuipes*" group (∼15% longer than HB), short or subequal in the "*spinosus*" group (∼40% longer than HB) and short or subequal in the "*paracou*" group (4% longer than HB). The ventral fur is golden, while it is completely white to pale orange in the "*tenuipes*" group, white to dull white in the "*spinosus*" group and pure white in the "*paracou*" group. The postglenoid foramen is very large, while it is small or medium in the groups "*tenuipes*" and "*spinosus*", and medium in the "*paracou*" group. It shares an undivided M1 anterocone with the "*paracou*" group, whereas it is divided in the groups "*tenuipes*" and "*spinosus*". The paralophule M1 is present, while it is absent in all other groups. Other differences are summarized in **Table** 3. All these morphological features indicate that Cordillera del Cóndor population does not belong to any previous recognized group, and it constitutes an own new group.

Morphometric analyses

The PCAs showed considerable overlap between species, but in the DFAs clear separation of species was achieved (**Fig**. 3). The first two principal components in the three analyses explained 61.13%, 67.56%, and 75.37% of the variation, respectively (**Table** 4); meanwhile, the DF1 explained from 52.56% to 64.14% of the variation in the DFA analyses (Figs. 3B, D, F). Species showed higher differentiation along the first PC and DF axes. In the DFA, the newly validated species *N. carceleni* is completely differentiated from *N. amoenus* (**Fig**. 3B). However, *N. carceleni* overlaps the most with *N. rosalindae* (**Figs**. 3E, F). The new species from Cordillera del Cóndor is easily differentiated from almost all the other species

Table 2
Uncorrected genetic p-distances in percentages (%) between species of *Neacomys*. The values in parentheses are the intraspecific species variations.

Species		1	2	3	4	5	6	7	8	9	10	11	12	13	14	15	16	17	18	19	20
1	*N. amoenus* (1.59±0.27)																				
2	*N. carceleni* (1.80±0.25)	3.26																			
3	*N. rosalindae* (1.10±0.14)	13.93	13.5																		
4	*N. minutus* up. river (0.89±0.19)	14.31	14.27	10.29																	
5	*N. musseri* (2.38±0.37)	13.23	14.31	11.2	12.72																
6	*N. paracou* (1.304±0.22)	14.37	14.09	13.8	14.86	15.26															
7	*N. dubosti* (0.73±0.15)	12.17	12.96	11.95	14.74	13.24	15.22														
8	*N. guianae* (0.89±0.26)	14.27	14.69	11.41	12.13	13.56	15.03	13.58													
9	*N. vargasllosai* (1.90±0.34)	8.86	8.33	12.47	13.51	12.36	13.02	13.35	14.01												
10	*N. spinosus* (1.02±0.44)	7.93	7.77	12.19	13.6	12.97	13.63	13.75	14.78	7.98											
11	*N. marajoara* (0.40±0.13)	12.09	12.37	12.44	12.47	13.63	13.4	9.44	13.26	12.74	13.9										
12	*N. xingu* (0.31±0.09)	12.76	12.74	12.49	11.79	13.02	14.58	10.19	13.43	13.01	14.62	4.02									
13	*N.* sp. clade 6 (2.83±0.47)	15.01	14.41	11.9	13.22	13.61	13.51	12.51	8.29	13.41	13.68	12.98	13.58								
14	*N. minutus* down river (0.69±0.13)	13.65	13.89	11.43	7.21	11.44	14.45	13.07	12.51	13.02	13.37	13.03	12.52	13.11							
15	*N. tenuipes* (4.66±1.14)	12.69	12.6	8.17	10.61	11.40	13.22	13.18	10.21	11.81	12.44	11.89	12.88	11.5	10.52						
16	*N. macedoruizi* n.a.	13.56	13.13	10.28	4.71	12.48	14.11	12.78	12.17	13.3	13.22	12.39	11.42	13.04	5.43	9.68					
17	*N. auriventer* sp. nov. (0.82±0.17)	11.8	12.89	12.85	14.09	13.6	14.23	12.91	14.94	14.3	12.26	13.70	13.22	13.44	12.85	13.51	13.33				
18	*N.* sp. 2 (0.59±0.17	12.8	12.54	13.08	13.84	13.52	15.29	10.86	14.15	13.37	14.18	8.86	7.23	12.42	12.17	13.96	13.37	12.78			
19	*N. minutus* down river	14.48	14.2	11.44	7.47	12.49	13.59	13.21	11.11	12.74	14.12	12.78	12.37	12.47	5.45	10.51	5.37	12.69	13.85		
20	*N. vossi* (0.52±0.17)	12.45	12.69	12.69	13.03	14.35	14.64	10.27	13.44	12.36	14.01	5.49	5.37	12.24	13.57	12.28	13.00	13.19	7.69	12.86	-

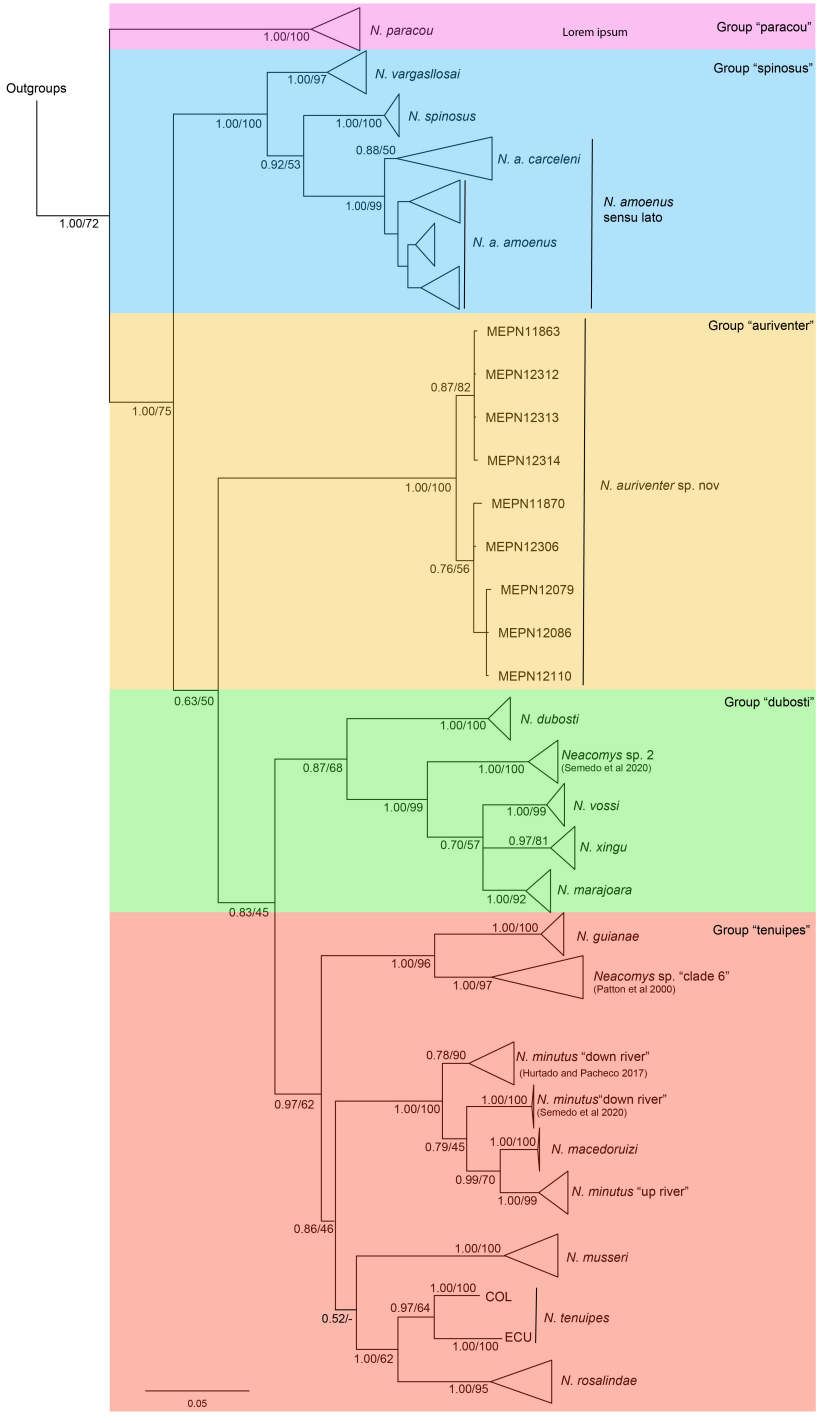

Fig. 1. Phylogeny of the genus *Neacomys* (Cricetidae: Sigmodontinae): Tree resulting from the Bayesian Inference analysis of the Cyt b gene. The numbers indicate Bayesian posterior probabilities (PP, left of the slash) and Maximum Likelihood bootstrap support values (BS, the right of the slash). Five clearly differentiated clades were observed, belonging to the groups: "*paracou*" (violet), "*spinosus*" (blue), "*dubosti*" (green), "*tenuipes*" (red) and the new group "*auriventer*" (yellow).

Table 3

Selected anatomical traits to distinguish morphologically groups of species recognized within *Neacomys*.

	"*paracou*"	"*spinosus*"	"*auriventer*"	"*tenuipes*"	"*dubosti*"
Body size	small (69-87 mm)	medium (72-102 mm)	small (64-75 mm)	small (62-99 mm)	small (62-88 mm)
Hind feet	large (18-22 mm)	large (19-26.5 mm)	large (20-24 mm)	small (17-28 mm)	small (13-26 mm)
Tail	short; subequal to larger than head-body length	short; subequal to 40% larger than head-body length	long; 55% larger than head-body length	short; 15% larger than head-body length	short; subequal to larger than head-body length
Pencil	absent	absent only in *N. carceleni*	present	absent	present
Ventral fur	often pure white	dull white to smoke white	orange	completely white to pale orange	pure white, yellowish white or buffy white
Rostrum	very short	large	large	short or large	notably broad
Postglenoid foramen	medium	small or medium	very large	small or medium	large
Subsquamosal fenestra	very small	small or large	large	small or large	small or large
Anterocone M1	undivided	divided	undivided	divided	undivided
Spur of enamel in M1	present	absent	absent	absent	absent
Paralophule M1	absent	absent	present	absent	absent
Source	Voss et al. (2001)	Hurtado & Pacheco (2017)	This study	Patton et al. (2000); Voss et al. (2001); Sánchez-Vendizú et al. (2018)	Semedo et al. (2020)

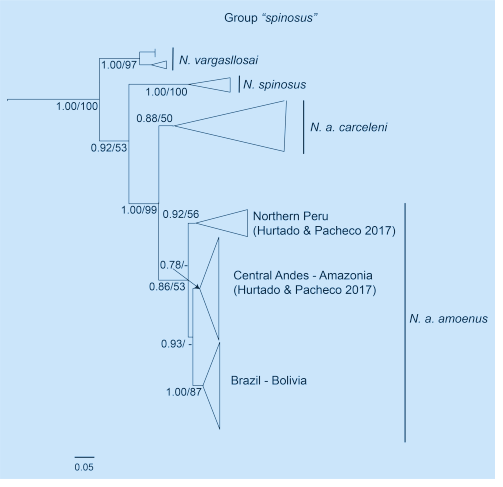

Fig. 2. Phylogeny of the group "*spinosus*" of genus *Neacomys* (Cricetidae: Sigmodontinae) Tree resulting from the Bayesian Inference analysis of the Cyt b gene. Numbers indicate Bayesian posterior probabilities (PP, left of the slash) and Maximum Likelihood bootstrap support values (BS, right of the slash).

included in the analyses, with the exception of *N. spinosus* (**Figs**. 3C, D).

The molecular and morphological data presented above indicate that the spiny mice from Cordillera del Cóndor represent a new species. We provide below a definition of the species, followed by a description and comparison with other congeneric forms and a discussion of its relationships. Also, we propose that *N. amoenus carceleni* should be recognized as a valid species and, therefore, treated as *N. carceleni* Hershkovitz, 1940, new combination. This species is present in the lower Amazon of Ecuador and Peru, while *N. amoenus* sensu lato is restricted to the north of the Amazon and the Central Andes of Peru, the southeast of Bolivia and the Amazon of Brazil.

Table 4

Percentage of explained variation and loadings of the first two principal components of the PCAs conducted on 5 species of *Neacomys*. Abbreviations of the measurements are explained in the text and **Table** S1 and PCAs are depicted in **Figs**. 3A, C and E.

		PCA (Fig. 3A)		PCA (Fig. 3C)		PCA (Fig. 3E)	
		PC1	PC2	PC1	PC2	PC1	PC2
	% Variation	49.84	11.29	54.47	13.09	67.22	8.37
1	CIL	0.9235	-0.1803	0.9533	-0.2459	-0.9611	0.0675
2	ZB	0.9017	-0.2303	0.9344	-0.0496	-0.9526	-0.0648
3	BB	0.6315	-0.4137	0.7196	0.1886	-0.8773	-0.2070
4	IOC	0.2647	-0.6433	0.3969	-0.2323	-0.6882	-0.2144
5	RL	0.6370	0.5535	0.5467	0.6644	-0.7862	0.1155
6	NL	0.7242	-0.2163	0.7827	-0.2312	-0.9042	-0.0139
7	RW-1	0.8167	-0.0663	0.8388	0.0801	-0.9127	-0.0852
8	OI	0.8859	0.3004	0.9171	-0.0438	-0.8568	0.3819
9	DL	0.8261	-0.2373	0.9203	-0.0313	-0.957	0.0206
10	MTRL	0.7131	0.0498	0.8551	-0.3198	-0.8853	-0.0293
11	IFL	0.7160	0.5356	0.7321	0.2703	-0.7717	0.1416
12	MB	0.4883	-0.1121	0.4062	0.5856	-0.8151	-0.3939
13	BOL	0.7329	-0.0966	0.7730	-0.0567	-0.7566	0.2599
14	MPFW	0.4403	0.5552	0.3724	0.161	0.2662	0.8496
15	ZPB	0.7891	0.0142	0.846	-0.4103	-0.8894	0.0859
16	CP	0.4025	0.1109	0.2654	0.8495	-0.5329	0.3184

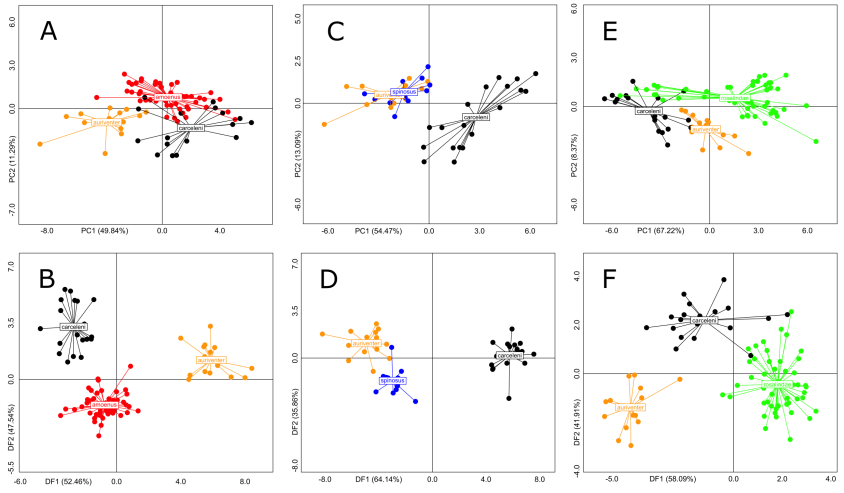

Fig. 3. Morphometric analyses of five species of *Neacomys*. A) Scatter plot of the PCA of *N. auriventer*, *N. carceleni* and *N. amoenus*. B) Scatter plot of the DFA of *N. auriventer*, *N. carceleni* and *N. amoenus*. C) Scatter plot of the PCA of *N. auriventer*, *N. carceleni* and *N. spinosus*. D) Scatter plot of the DFA of *N. auriventer*, *N. carceleni* and *N. spinosus*. E) Scatter plot of the PCA of *N. auriventer*, *N. carceleni* and *N. rosalindae*. D) Scatter plot of the DFA of *N. auriventer*, *N. carceleni* and *N. rosalindae*.

Taxonomy

Subfamily Sigmodontinae Wagner, 1843
Tribe Oryzomyini Vorontsov, 1959
Genus *Neacomys* Thomas, 1900
Neacomys auriventer sp. nov.
Golden-belly Spiny Mouse
Ratón espinoso de vientre dorado
LSID: urn:lsid:zoobank.org:pub:20E8EF9E-2486-4F76-8B7F-7DBA891CD6DA

Holotype

An adult male (MEPN 12081) preserved as skin, skull, postcranial skeleton and a tissue sample, collected on September 11, 2011 by Alfonso Arguero.

Paratopotypes

A young male (MEPN 12078) and an adult female (MEPN 12079) collected on September 10, 2011 by A. Arguero; two adult males (MEPN 11846, 11863)

collected on October 23 and 28, 2010, and two adult females (MEPN 11854, 11870) collected on October 24 and 30, 2010 by A. Arguero, and Angel Angamarca; four adult males (MEPN 12306, 12312-14) collected on July 15, by Marilyn Novillo; an adult female (MEPN 12557) collected on October 9, 2014 by Alejandro Mesías.

Paratypes

Two adult males (MEPN 12086–87) collected on September 21, 2011, and an adult female (MEPN 12110) collected on May 1, 2012 by A. Arguero and Angel Angamarca in the Refugio de Vida Silvestre El Zarza (3°48'18.16"S, 78°30'24.24"W, 1,460 m), Parroquia Los Encuentros, Cantón Yantzaza, Province of Zamora Chinchipe, Ecuador; two adult males (MEPN 12485, 12306) collected on January 29, 2014 by A. Mesías in Las Peñas (3°46'36.46"S, 78°29'44.59"W, 1,633 m), Parroquia Los Encuentros, Cantón Yantzaza, Province of Zamora Chinchipe, Ecuador; an adult male (MECN 5420) collected on November 19, 2016 by Janina Bonilla in Tundayme (3°34'44.1"S, 78°24'45.4"W, 1,729 m); and an adult male (MECN 5423) collected on November 5, 2016 by Rubí García in Tundayme (3°34'54.6"S, 78°24'37.9"W, 1,885 m), Parroquia El Pangui, Province of Zamora Chinchipe, Ecuador.

Type locality

Paquisha Alto (3°55'4.12"S, 78°29'33.78"W, [coordinates taken by GPS at the trapsite], 1,885 m), Parroquia Paquisha, Cantón Paquisha, Province of Zamora Chinchipe, República del Ecuador.

Diagnosis

A species of *Neacomys* with the following combination of characters: small size (head-body length ~69 mm); tail long (55.5% longer than head and body length); belly fur golden; postglenoid foramen very large; M1 anterocone undivided; presence of paralophule on M1; M1-M3 and m1-m3 with reduced labial and lingual cusps, respectively; mesoloph in M1 wide; hypoflexus in M2 wide and tilted towards the metacone; mesoflexid in m1 large; posterolophid in m1 wide with hypolophulid; hypoflexid in m2 wide and tilted towards the posteroflexid.

Morphological description

The following description was based on all specimens available. *Neacomys auriventer* sp. nov. is a spiny mouse of small size (head and body length=64-75 mm). The dorsal pelage is dark brown; soft hairs are mixed with spines; in average dorsal hairs are 10 mm in length. The soft hair is tricolor, with a black band at the base, a light brown band in the middle and a black apical band. The posterior mystacial vibrissae are thick and long (29-39 mm), surpassing the auricular pinnae when adpressed back; two superciliary vibrissae (18-32 mm) are present. Two medium-sized genal vibrissae (27-32 mm) are also present, which are more slender than the mystacial vibrissae. The two interramal vibrissae (5-6 mm) are inserted at a basal protuberance. The ears are small (12-15 mm) and oval in outline. Although the ears seem to be Naked, they are covered with short yellow hairs. The base of the internal ears is pale yellowish and the edges are dark, the hairs are black and medium in size. A small pale orange postauricular patch is present. The pelage on the throat is orange and extends up to the corners of the mouth. The ventral pelage is golden (**Fig**. 4), and the hairs are on average 5 mm in length at the middle of the belly. The ventral hairs are bicolored with the basal half gray and the apical half golden. The tail is uniformly dark, slender and long (51.1-55.5% longer than head and body length). It is covered with squared scales (16-18 rows/cm near the base), with dark-brown hispid three hairs emerging from the base of each scale, not longer than 1.5-2 scale rows. The hairs of the terminal portion of the tail form a small tuft (<5 mm). Females have eight mammae arranged in pectoral, toraxic, abdominal and inguinal pairs.

The manus is slender and short. The first digit is reduced with a short and wide claw. The other claws are short and curved. Ungual tufts are white and extend beyond the claw ends. The dorsal surface has a patch at the level of the metacarpal bones, with evident brown scales; each scale has three dark brown hairs and sometimes the central hair is the longest. Long carpal vibrissae, can extend beyond the second interphalangeal of digit V. The digits are relatively large; digit I is substantially shorter than digit II; digit II is shorter than digit III; digit III is slightly larger than digit IV; digit IV is larger than digit V (**Fig**. 5). Hind feet are long and slender (20-24 mm); the ungual tufts are white and extend slightly beyond the tip of claws. Their dorsal surface has an ample metatarsal patch, with conspicuous brown scales (**Fig**. 5); each scale has three dark brown hairs. Large number of granules covers the most of the plantar surface, including the spaces between the pads and reaching the anterior border of the thenar pad. The four interdigital pads are elevated and similar in size; pads two and three are separated by a small interspace, while pads two and four are separated by an interspace of similar size than pad

Fig. 4. *Neacomys auriventer* sp. nov. (Cordillera del Cóndor, Ecuador). Top: adult male paratype (MEPN 12312), external aspect in live. Bottom: dorsal and ventral views of adult male holotype (MEPN 12081). Scales = 10 mm.

one (**Fig**. 5). The hypothenar pad is small, while the thenar pad is well developed, large and elevated anteriorly. Digits are relatively short; digit I reaches the base of digit II; digit II is slightly shorter than digit III; digit III is slightly larger than digit IV; digit IV is larger than digit V; digit V reaches the distal end of the first phalanx of digit IV (**Fig**. 5); claws short, unusually recurved, basally opened, except the pollex which bears a Nail.

The cranium is moderately large for the genus (average CIL=19.2 mm) with the braincase showing a convex profile (**Fig**. 6). Dorsal profile of cranial roof is flat from nasal to parietals to slope gently downward toward occiput; the rostrum is short; premaxillae slightly shorter than nasals not extending anteriorly beyond incisors without forming a rostral tube; gnathic process is very small; the suture between the nasal bones and the premaxillary reaches the root of the zygomatic bone; the nasal bone is narrow at the base and gradually widens forward; the interorbital region is narrow; the supraorbital edges are small and sharp; the zygomatic notches are shallow and wide while seen from above; in the olfactory sagittal plane are present two fronto-turbinals, one interturbinal and three ethmoturbinals (**Fig**. 7E); the lachrymal is small, with contact in equal proportions with the frontal and maxillary; the fronto-parietal suture is V-shaped; the braincase is rounded and inflated; the zygomatic plate is wide (> M1 length) and slightly inclined forward;

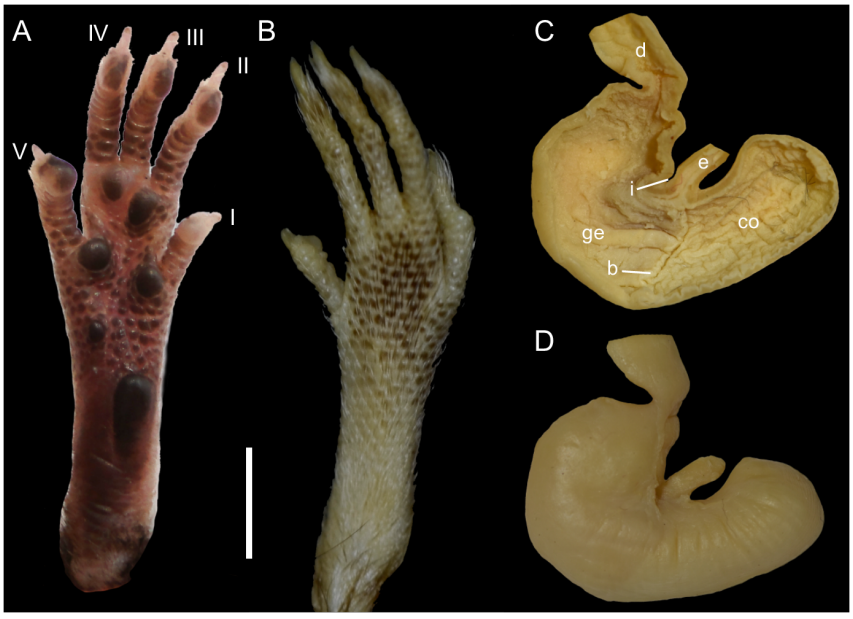

Fig. 5. Ventral (A) and dorsal (B) views right of the hind foot of the adult male paratype of *Neacomys auriventer* sp. nov. (MEPN 12312; Cordillera del Cóndor, Ecuador), and internal (C) and external (D) views of the stomach of the same individual. Abbreviations: I-V = digits, b = bordering fold, co = cornified epithelium, d = duodenum, e = esophagus, ge = glandular epithelium, i = incisura angularis. Scale = 5 mm.

in the zygomatic arch a small jugal is present; a squamosal-alisphenoid groove is visible through the translucent braincase, with a perforation where it crosses the depression for the masticatory nerve; the stapedial foramen is present and small, carotid canal small, and expressed petrotympanic fissure (**Figs**. 7B, D); the cephalic arterial supply is primitive (pattern 1 of Voss 1988); the alisphenoid strut is absent (**Fig**. 7C); anterior opening of alisphenoid canal is present and small (**Fig**. 7C); the postglenoid foramen is very large; the subsquamosal fenestra is large and the hamular process of squamosal is long (**Fig**. 7A); a well-developed tegmen tympani is present; the auditory bullae are large, being the stapedial process of bulla small but the meatus broad; the paraoccipital process is broad (**Figs**. 7A, D). The Hill foramen is tiny; the incisive foramina are short and wide, ending well anterior to the M1s anterior faces; the capsular process of premaxillary is well developed; the palate is wide and long with the anterior border of the mesopterygoid fossa not reaching M3s posterior faces; the palatal foramina are small and numerous; the posterolateral pits are long and paired, and located parallel to anterior part of the mesopterygoid fossa; the mesopterygoid fossa is broad as the parapterygoid plates, with the anterior margin ⋂-shaped; the sphenopalatine vacuities are elongated, occupying most of the presphenoid area; the presphenoid is wide; the Eustachian tube is small and has no contact with the pterygoid plate; the petrosals are well-exposed (**Fig**. 7D).

The mandible with masseteric crest below the procingulum of m1; the coronoid process is small, slender, and bended backwards; the sigmoid notch is oval; the condylar process is large and robust; the angular notch is shallow, and the angular process is blunt (**Fig**. 6).

The incisors are ophistodont, without grooves, and with orange enamel. (**Fig**. 6); the molars are brachydont and terraced (**Fig**. 8); the main cusps of the upper molars are opposed, while those of the lower molars are in a slightly oblique design.

The M1-M3 have small labial cusps (**Fig**. 8); the M1 is rounded in outline; the procingulum is narrower than the rest of the molar, with a rounded anteromedian fossette present; a paralophule and a spur of enamel are also presents (**Fig**. 8); the mesoflexus is small; the metaflexus is large and wide; the mesofossette is large; the posteroloph is large. The M2 has a slim and reduced protoflexus; the anteroloph is very small; the mesoflexus is short and wide; the mesoloph is short; the mesofosette is

Fig. 6. Skull of the holotype of *Neacomys auriventer* sp. nov. (MEPN 12081; Cordillera del Cóndor, Ecuador) in dorsal, ventral, and lateral views. Scale = 5 mm.

rounded; the posteroloph is similar to M1. The M3 has a small paraflexus and shallow hypoflexus. The upper molars have three roots each. The m1-m3 have small lingual cusps (**Fig**. 8). The m1 is rectangular m1 in outline; the procingulum is not divided into labial and lingual conulids; the protoflexid is short and slender; the hypoflexid is short and wide; the mesoflexid is large; the metaconid has a metalophid; the mesolophid is large; the posteroflexid is short, broaden and with a hypolophulid; the mesofosette is large. The protoflexid in m2 is small and short; the hypoflexid is wide and inclined with direction towards the posteroflexid; the mesoflexid is short and slender; the mesolophid is short and wide; the mesofosette is large. The m3 is anteriorly-posteriorly compressed, having a wide hypoflexid is wide and a well developed anterolabial cingulum and a protoflexid. The lower molars have two roots each.

The gall bladder is absent (four specimens examined: MEPN 11854, 11870, 12306, 12312). The stomach (four specimens examined: MEPN 11854, 11870, 12306, 12312) is unilocular and hemiglandular; the cornified epithelium lines the corpus and shows a noticeable wrinkled aspect, while the glandular epithelium occupies the antrum and is slightly extended to the left of the esophageal opening; the bordering fold is notorious for being thick and long, surpassing the left level of the incisura angularis; the incisura angularis is moderately deep and the plica angularis is well expressed with a well-developed pars pyloricus (**Fig**. 5).

Measurements of the holotype (in mm): Head and body length=75, tail length=117, hind foot length (including claw)=22, ear height=15, length of longest mystacial vibrissae=29.5, length of longest superciliary vibrissae=29.9, length of longest genal vibrissae=31.24, body mass (in grams)=17, condylo-incisive length=19.9, length of upper diastema=6.1, length of palatal bridge=4.05, crown length of maxillary toothrow=2.8, length of incisive foramen=3.2, breadth of mesopterygoid foramen=1.42, breadth of rostrum=7.07, length of rostrum=7.1, length of nasals=7.9, length of palatal bridge=4.4, least interorbital breadth=4.5, zygomatic breadth=11.8, breadth of zygomatic plate=1.8, orbital fossa length=7.1, breadth of braincase=10.9, cranial depth=8.3, mastoid breadth=10.3, length of basioccipital=3.1, length of mandible=11.2. External and craniodental measures of additional specimens are listed in **Table** 5.

Taxonomic comparisons

Neacomys auriventer is the only known species within the genus *Neacomys* that combines a small size (head-body length 64-75 mm), tail much longer than head-body (80-119 mm), and golden ventral coloration (see Pardiñas et al. 2017; Sánchez-Vendizú et al. 2018; Semedo et al. 2020). These external traits are useful to identify this species with confidence. In the following paragraphs, we discuss additional characters to distinguish *N. auriventer* from other con-

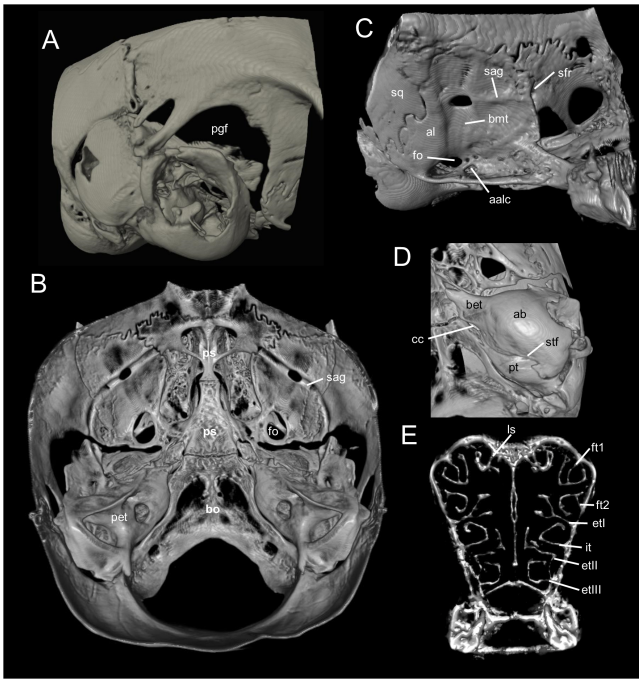

Fig. 7. Selected aspects of qualitative anatomy in the cranium of the holotype of *Neacomys auriventer* sp. nov. (MEPN 12081; Cordillera del Cóndor, Ecuador), scaled to the same length. A, right temporal region in lateral view; B, dorsal view of the basicranial region (roofing bones of braincase removed); C, right squamosal-alisphenoid region in lateral view; D, left auditory capsule in ventral view; and E, 3D representations of turbinal bones. Abbreviations: aalc = anterior opening of alisphenoid canal, ab = auditory bulla (ectotympanic), al = alisphenoid, bet = bony eustachian tube, bmt = trough for masticatory-buccinator nerve, bo = basioccipital, bs = basisphenoid, cc = carotid canal, etI = ethmoturbinal I, etII = ethmoturbinal II, etIII = ethmoturbinal III, ft1 = frontoturbinal 1, ft2 = frontoturbinal 2, fo = foramen ovale, it = interturbinal, ls = lamina semicircularis, pet = petrosal, pgf = postglenoid foramen, ps = presphenoid, pt = petrosal, sag = squamosal alisphenoid groove, stf = stapedial foramen, sfr = sphenofrontal foramen, sq = squamosal.

geners (character states of other *Neacomys* species are given between parentheses).

N. auriventer differs from *N. tenuipes* by having longer tail than HB ∼55% (15%); a small and inconspicuous lachrymal (big and visible); uninflated nasolacrimal capsules (inflated); a broad and deep zygomatic notch while seen from above (narrow and deep); bottle-shaped otic bullae, which are broader at the posterior end and narrower at the anterior end (flask-shaped).

N. auriventer is different from *N. amoenus* by having ungual tufts that extend beyond the claws (do not extend beyond the claws); a large metacarpal patch, with scales and dark hairs (absent); thin and long genal vibrissae, which extend beyond the pinna (short, do not extend over the posterior margin of the pinna); a tail length ∼55% longer than head-body length, and tail ends in a small tuft 5 mm (the tail does not end in a brush); an "U" shaped anterior border of the foramen magnum ("V" shaped); a narrow mesopterygoid fossa bearing a palatine spine process (wide and without palatine spine).

N. auriventer is different from *N. carceleni* by having a golden ventral coloration with grey at the base (completely white); a yellowish orange postauricular patch (bright orange); a large metacarpal patch (small); short carpal vibrissae, reaching to the base of the fifth digit (long, passing the second interphalangeal joint of the fifth digit); a rounded and inflated skull (more flat and elongated); weakly developed and dorsally oriented supraorbital crests (strongly developed, dorsolaterally oriented and expanded supraorbital crests); shallow zygomatic notches (deep); a narrow mesopterygoid fossa (wide); an "U" shaped anterior border of the foramen magnum ("V" shaped); a narrow and short condylar process (broad and short); an open sigmoid notch (closed); a slightly shorter metaflexus of M1, not reaching the labial margin (long, extending beyond the labial margin); a narrow anteroloph of M2, reaching the labial surface (broad and does not reach the labial surface).

N. auriventer differs from *N. vargasllosai* by having long carpal vibrissae, that could extend beyond the second interphalangeal joint of digit V (short, extending the first interphalangeal joint of digit V); a narrow mesopterygoid fossa, with a small posterolateral palatal pit (wide and with developed posterolateral palatal pit); absence of a fontanelle perforating the pterygoid plate (present); auditory bullae, which are wide in the posterior region and narrow in the anterior region (flask-shaped); a "⋂" shaped anterior border of the foramen magnum ("∧" shaped); molars with opposed conules (slightly); a short and superficial protoflexus of M1 (large and deep); a short hypoflexid of m1 which is perpen-

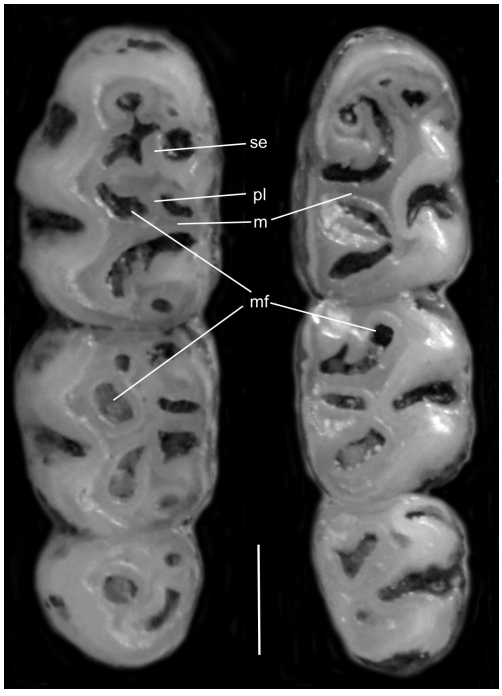

Fig. 8. Occlusal view of right upper (left) and lower (right) toothrow of the holotype of *Neacomys auriventer* sp. nov. (MEPN 12081; Cordillera del Cóndor, Ecuador). Abbreviations: m = mesoloph/id, mf = mesofossette/id, pl = paralophule, se = spur of enamel. Scale = 0.5 mm.

dicular to the median mure (large and oblique); a narrow anterolabial cingulum of m2 (wide); a short hypoflexid of m2 which is oblique to the median mure (large and perpendicular); a wide mesoflexid of m3 (small).

N. auriventer is different from *N. spinosus* by lacking a metatarsal patch (present); a tail length 55% longer than head-body length (20%); a rounded and inflated skull (more flat and elongated); the suture between the nasal and the premaxillary reaching the root of the zygomatic (does not reach the root of the zygomatic); small posterolateral palatal pits (enlarged); long sphenopalatine vacuities, with the anterior region wide while the posterior region is narrow (long but with wide posterior region); absence of alisphenoid strut (present); a long and narrow lacerate foramen (long and wide); an oblique and narrow paraflexus of M1 (parallel to the median mure and wide); a short paraflexus, like a dimple, which does not reach the labial margin (long and reaches the labial margin); a metaflexus which is divided in two fossettes that do not reach the labial margin (long and reaches the labial margin); a long and narrow metaflexid of m1 (short and wide); a short and deep hypoflexid, which does not reach the median mure (long and superficial, reaches the median mure); a narrow anterolabial cingulum of m2 (wide); a short, narrow, and oblique hypoflexid of m2 (long, wide and perpendicular to the median mure).

Table 5

External and cranial measurements (in mm) and weight (in grams) of adults of *Neacomys auriventer* sp. nov. The values provided are observed range, (mean±standard deviation) and sample size.

	Males	Females
Head and body length	66-75 (70±3.3) 8	64-75 (69.3±4.6) 4
Tail length	80-119 (105.8±14.1) 8	101-117 (107.8±7.6) 4
Hind foot length (including claw)	20-24 (22.2±1.5) 8	20-24 (22±1.6) 4
Ear length	12-15 (13.5±1.5) 8	13-14 (13.8±0.5) 4
Longest mystacial vibrissae	29.6-38.3 (33.9±3.9) 8	29.4-39.8 (34.2±4.3) 4
Length of longest superciliary vibrissae	26-31.3 (29.3±1.8) 8	25-30.4 (27.9±2.3) 4
Length of longest genal vibrissae	27.3-32.5 (29.5±3.4) 8	29.6-31.4 (30.5±15.3) 4
Body mass	13-18 (16.1±1.9) 8	12.5-13 (12.8±0.4) 4
Condylo-incisive length	18.06-20.4 (19.5±0.6) 11	17.8-20 (18.9 ±0.9) 4
Length of upper diastema	3.9-6.3 (5.5±0.8) 11	5.1-5.9 (5.5±0.4) 4
Crown length of maxillary toothrow	2.7-2.9 (2.8±0.1) 11	2.7-2.8 (2.7±0.07) 4
Length of incisive foramen	2.7-3.2 (3.04±0.1) 11	2.1-3.1 (2.6±0.4) 4
Breadth of foramen mesopterygoid	1.2-1.8 (1.5±0.1) 11	1.2-1.4 (1.3±0.08) 4
Breadth of rostrum	3.9-4.3 (4.1±0.1) 11	3.9-4.1 (4.1±0.1) 4
Length of rostrum	6.4-7.1 (6.9±0.2) 11	6.4-6.8 (6.6±0.2) 4
Length of nasals	7.8-8.8 (8.2±0.4) 11	8.02-8.7 (8.3±0.4) 4
Least interorbital breadth	4.2-4.7 (4.4±0.1) 11	4.3-4.8 (4.6±0.1) 4
Length of palatal bridge	4.04-4.1 (4.1±0.04) 6	-
Mastoid breadth	9.2-10.2 (10±0.2) 11	9.4-10.1 (9.9±0.3) 4
Length of basioccipital	2.6-3.2 (3.1±0.2) 11	2.9-3.2 (3.1±0.1) 4
Cranial depth	7.5-8.6 (8.2±0.3) 11	7.6-8.4 (8.04±0.3) 4
Zygomatic breadth	11.1-12.1 (11.6±0.3) 11	10.3-11.6 (11.1±0.5) 4
Breadth of zygomatic plate	1.6-2 (1.8±0.1) 11	1.6-1.9 (1.7±0.1) 4
Orbital fossa length	6.2-7.3 (6.9±0.3) 11	6.1-6.8 (6.6±0.3) 4
Breadth of braincase	10.7-11.1 (10.9±0.1) 11	10.4-11.2 (10.8±0.3) 4
Length of mandible	10.6-11.4 (11±0.3) 8	10.3-11.2 (10.7±0.4) 4

N. auriventer can be easily separated from *N. rosalindae* (Sánchez-Vendizú et al. 2018) by having a tail much longer than HB, ∼55% (slightly longer tail than HB, ∼2%); golden ventral fur (pure white) (**Fig**. S2); tail with 16-18 caudal scale rows per centimeter (17-24); postglenoid foramen very large (large).

Additional comparisons among the species are presented in **Table** 6.

Etymology

The specific epithet *auriventer* comes from the Latin aureus=golden, and venter=belly, highlighting to the noticeable coloration of the ventral fur.

Table 6
Comparison of *N. auriventer* sp. nov. with selected *Neacomys* species.

Character	*N. auriventer*	*N. rosalindae*	*N. vargasllosai*	*N. spinosus*	*N. carceleni*	*N. amoenus*
Dorsal fur color	Dark brown	Deep orange	Dark brown	Reddish brown	Pale orange brown	Pale orange brown
Flanks of fur	Yellowish orange	Pale yellow	Narrow and yellowish orange	Reddish	Pale ochraceous	Pale yellowish
Ventral fur color	Golden with gray base	Completely white or slightly buffy	White with gray base	White with dark gray base	Completely white	White with gray base
Genal vibrissae	Pass posterior border of the pinna	Pass posterior border of the pinna	Do not pass posterior border of the pinna	Pass posterior border of the pinna	Do not pass posterior border of the pinna	Do not pass posterior border of the pinna
Metatarsal patch	Absent	Present	Absent	Present	Absent	Absent
Tail	55% larger than head-body length	2% larger than head-body length	40 % larger than head-body length	20 % larger than head-body length	Subequal to head-body length	5% larger than head-body length
Pencil	Present	Present	Present	Present	Present	Absent
Rostrum	Short and narrow	Short	Narrow and laterally flat	Broad and tapering	Broad and tapering	Broad and truncated
Gnathic process	Short	Short	Short	Short	Large	Short
Zygomatic notch	Slightly deep and wide seen from above	Short and shallow	Shallow	Shallow	Shallow	Deep
Lacrimals	Small and narrow	Usually conspicuous and rounded	Squared, one half dip in the frontal	Rounded, two-thirds dip in the frontal	Squared, one half dip in the frontal	Rounded, two-thirds dip in the frontal
Inner borders of the incisive foramina	Anteriorly convergent	Posteriorly parallel	Posteriorly convergent	Posteriorly parallel	Posteriorly parallel	Posteriorly convergent
Diastema	Flat	With a small hump	Flat	Flat	With a small hump	Flat
Eustachian tube	Short	Short	Short	Short	Large	Large
Bullae	Bottle-shaped	Flask-shaped	Flask-shaped	Globular	Globular	Globular
Anterior bullae process	Not in contact with the pterygoid plate	Not in contact with the pterygoid plate	Not in contact with the pterygoid plate	Almost in contact with the pterygoid plate	In contact with the pterygoid plate	Not in contact with the pterygoid plate
Anterior border of the foramen magnum	Rounded U shaped	Obtuse V shaped with a moderate notch	Obtuse V shaped with a moderate notch	Obtuse V shaped	V shaped with a small notch	Obtuse V shaped
Molar rows	Posteriorly convergent	Parallel	Parallel	Parallel	Posteriorly convergent	Parallel
Antero median flexus of M1	Does not reach labial surface	Does not reach labial surface	Does not reach labial surface	Reaches labial surface	Does not reach labial surface	Reaches labial surface

Distribution and natural History

Specimens of *N. auriventer* were recorded in four localities of the Cordillera del Cóndor in Ecuador (**Fig**. 9, **Table** S3). It lives in the mountain rainforests, between 1 460-1 885 m. The zone corresponds to the Eastern Mountain Forest (Ministerio Del Ambiente del Ecuador 2013), in the zoogeographic regions Eastern Subtropical and Temperate(Albuja et al. 2012). The specimens were captured on the ground level, where the forest canopy is at 10 to 20 m, with emerging trees that reach up to 25 m. Trees are covered with abundant climbing plants, epiphytes, ferns, hemiepiphytes and mosses. Above 1 700 m, the forest floor has entangling roots and abundant litter, forming a false floor locally known as bamba (Jadán

& Aguirre 2011; Almendáriz et al. 2014). *N. auriventer* was registered in sympatry with *Akodon aerosus*, *Hylaeamys tatei*, *Oecomys bicolor*, *Rhipidomys* sp., and *Thomasomys pardignasi*.

Conservation status

We consider that *N. auriventer* should be classified as Endangered (EN), following the criteria B1a, b(i,ii,iii) of the IUCN (2012). The main reasons to support the advanced status are: (1) it is estimated that the extension of its distribution is less than 100 km^2, and (2) it has only been found in four localities in the province of Zamora Chinchipe, which are all within areas of a mining concession (ARCOM 2015; Roy et al. 2018), and two localities are severely affected by large operations of open-pit mining (**Fig**. 10). The latter causes habitat loss (mainly deforestation), produces a population decline, and increases the risk of local extinctions as it has been reported for the frog species *Pristimantis zantzaza* (Valencia et al. 2017) and *Hyloscirtus hillisi* (Ron et al. 2018) which are sympatric with *N. auriventer*. In addition, habitat disturbance increases the risk of introducing invasive species that displace native species and can easily tolerate habitat changes, such as: the black rat *Rattus rattus*, the brown rat *R. norvegicus*, and the house mouse *Mus musculus* (Dowler et al. 2000; Mena et al. 2007).

Neacomys carceleni Hershkovitz, 1940, new combination

Neacomys carceleni Hershkovitz, 1940
Alberto Carcelén's Spiny Mouse
Ratón espinoso de Alberto Carcelén
Neacomys spinosus carceleni Hershkovitz, 1940:1
Neacomys amoenus carceleni: Hurtado and Pacheco, 2017, name combination

Holotype

An adult male (UMMZ 80171); skin, and skull, collected on October 5, 1936 by P. Hershkovitz.

Type locality

"Llunchi, an island on the northern side of the Rio Napo, west of the mouth of the Rio Jivino, latitude and longitude approximately 0°37' S., 76° 46' W.; parish of La Coca, Napo-Pastaza Province, Ecuador; altitude about 250 meters" (Hershkovitz 1940:1).

Distribution

Neacomys carceleni occurs from 200 to 1 885 m (Hurtado & Pacheco 2017; **Fig**. 9 and **Table** S3) in Eastern Ecuador, in the provinces of Napo, Morona Santiago, Tungurahua, Orellana, Pastaza, Sucumbíos, Zamora Chinchipe; and in Peru, in the departments of Loreto, Madre de Dios and Ucayali (**Fig**. 9; Hurtado & Pacheco 2017).

Emended diagnosis

The external and cranial characters that allow *N. carceleni* to be considered as a separate species from *N. amoenus* (character states between parentheses) are: completely white and short ventral fur (white with gray base); long ungual manus tufts and carpal vibrissae (short not surpassing the claws); short hind feet (large); absent tuft of caudal hairs (5% larger and present); broad and tapering rostrum (broad and truncated); large gnathic process (short); squared lacrimals, one-half dip on squamosal root of zygomatic bone, and one-half in the frontal bone (rounded, one-half is inserted on the squamosal root of zygomatic); posteriorly convergent upper molar rows (parallel); upper diastema with a hump (flat); anterior otic bulla process being in contact with pterygoid plate (not in contact); deep basioccipital pits (shallow); masseteric crest of the jaw being below the hypoconid of m1 (below the procingulum); an asymmetrically divided anteroloph of M1 (symmetrically divided); a straight posterior border of posteroloph of M1 (convex); and a broad anterolabial cingulum of m2 (narrow).

For a detailed description of *N. carceleni* see Hurtado & Pacheco (2017).

DISCUSSION

The genus *Neacomys*–with the description of *N. auriventer* sp. nov. and the validation of *N. carceleni*–currently comprises 17 species. Despite the general impediments and problems that taxonomic research faces (e.g., Britz et al. 2020; Dupérré 2020), the recent advances in the taxonomy of this genus show a promising trend. The first species was described in 1882, and a handful of species and subspecies were described until 1940 (Weksler & Bonvicino 2015). Later, there was a gap of six decades between the description of *N. carceleni* by Hershkovitz (1940) and the descriptions of *N. musseri* and *N. minutus* by Patton et al. (2000). Interestingly, most of the species of *Neacomys* have been described in the 21st century, two species by Patton et al. (2000), two by Voss et al. (2001), one by Hurtado & Pacheco (2017), two by Sánchez-Vendizú et al. (2018), and, very recently, three by Semedo et al. (2020).

The high number of species, even for a genus of oryzomyine rodent, makes *Neacomys* an interesting

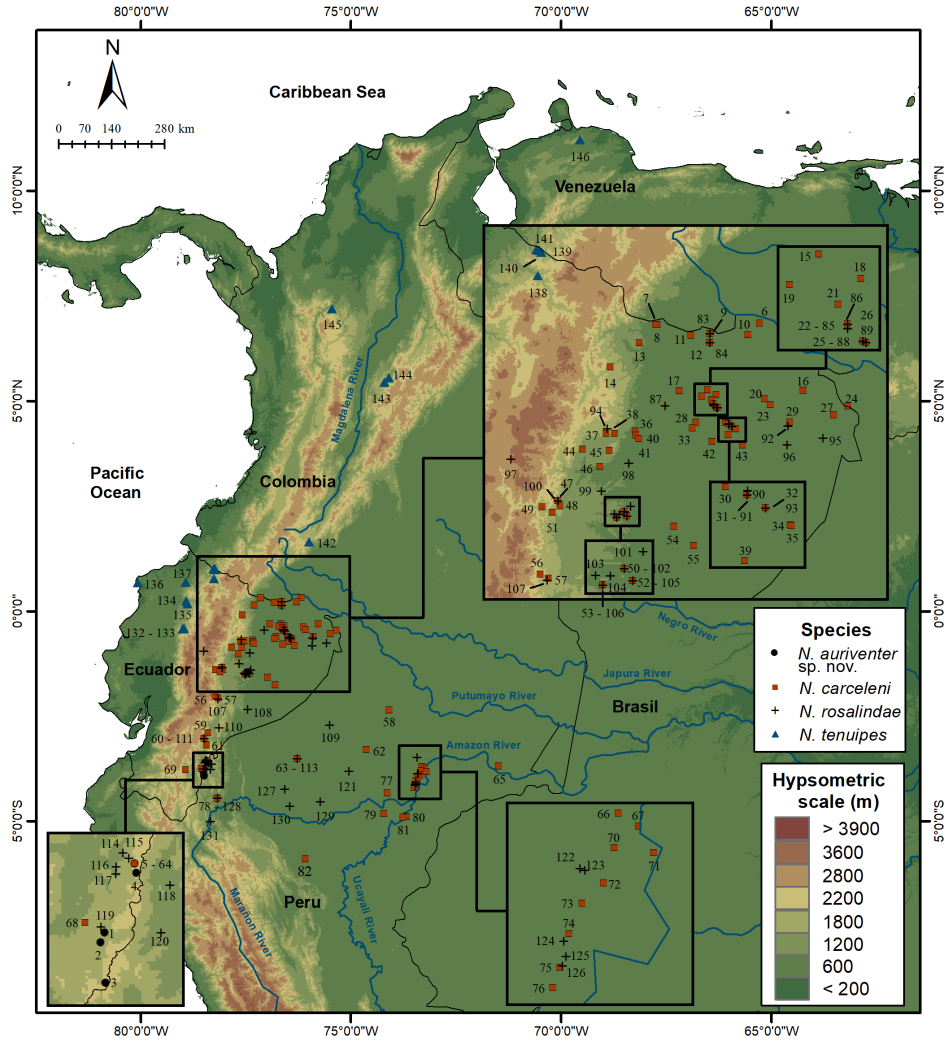

Fig. 9. Map of northwestern South America depicting recording localities for the species of *Neacomys* associated with *Neacomys auriventer* sp. nov. Number of sites according to **Table** S3.

model for historical biogeography and evolutionary studies. With its ample Amazonian and Trans-Andean distribution, the genus could be used to explore traditional biogeographical patterns like area relationships of Neotropical lowland forests (e.g., Ron 2000) and–because of its high diversity in the Amazon–the Pleistocene Refuge Hypothesis (Haffer 1969; but see Lessa et al. 2003) and the Riverine Barrier Hypothesis (Wallace 1849), expanding on the classic works of Patton et al. (1994, 2000). In addition, the peculiar natural history of *Neacomys*, which is a genus of small and fully terrestrial mice, makes it appealing as a contrasting model for comparisons with other Neotropical genera such as *Oecomys*, which is also a speciose oryzomyine but arboreal.

The phylogenetic analyzes confirmed *Neacomys* as monophyletic and constituted by five groups of species: the four groups previously described (i.e., "*dubosti*", "*paracou*", "*spinosus*", and "*tenuipes*"), and the new added here, "*auriventer*" group. The sole member of the latter, *N. auriventer* is restricted to the Cordillera del Cóndor in Eastern Ecuador, located to the south-east in the provinces of Morona Santiago and Zamora Chinchipe. This cordillera is delimited

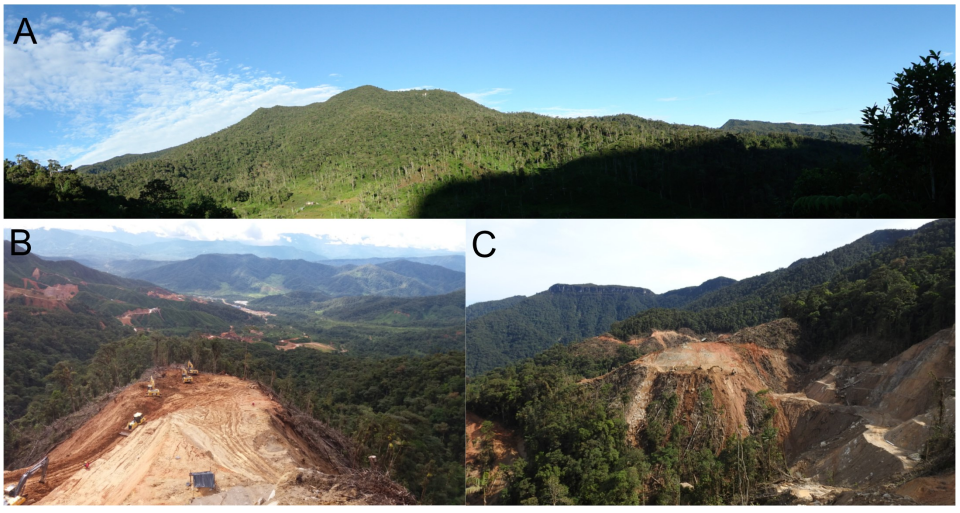

Fig. 10. Habitat of *Neacomys auriventer* sp. nov. in Cordillera del Cóndor, Ecuador: A, Paquisha Alto, the type locality; B and C, intensive habitat destruction and forest fragmentation for mining activities at Tundayme.

by two large rivers–Zamora and Santiago–which form deep gullies that could function as geographical barriers. It is possible that a population of an ancestral *Neacomys* was isolated between these rivers, giving origin to what is now *N. auriventer*. This pattern of isolation, either by dispersal or vicariance, could also be responsible for the origin of other endemic vertebrate taxa of the region, like the shrew opossum *Caenolestes condorensis*, and the frogs *Centrolene condor*, *Excidobates condor* and *Pristimantis barrigai* (Albuja & Patterson 1996; Almendáriz et al. 2014; Brito & Almendáriz 2018).

In general, the morphometric differentiation between species of *Neacomys* is unclear, which is not surprising for cryptic species (e.g., Granjon 2005; Yazbeck et al. 2011). Given the amount of genetic distinction and the sympatric distribution of some species of *Neacomys* (**Fig**. 9), the morphometric and morphologic similarities could be the result of niche conservatism (Wiens & Graham 2005; Losos 2008; Wiens et al. 2010). Although, it is striking how different *N. carceleni* is from other *Neacomys* and particularly from other species in the "*spinosus*" group. This distinctiveness supports the recognition of *N. carceleni* as a valid species.

N. carceleni was described by Hershkovitz (1940) as a subspecies of *N. spinosus*. However, our lines of evidence reveal that the differentiation of these taxa compared with all *Neacomys*, and particularly with *N. amoenus* sensu lato, is strong enough to warrant the species status of *carceleni*, despite low genetic distances. The morphological features (**Table** 6), morphometric distinction (**Fig**. 3), monophyly (**Fig**. 2), and its distribution (Hurtado & Pacheco 2017; **Table** S3) allow to *N. carceleni* to be considered as a full species. These multiple lines of evidence agree with the integrative taxonomy framework (e.g., Vieites et al. 2009; Padial et al. 2010).

The distribution of the species within the "*spinosus*" group suggests that the large Amazonian rivers may serve as geographical barriers. The distribution of *N. carceleni* is limited to the northwest by the Andes and the Napo River (Ecuador), and to the south by the Marañon River and the Ucayali River (Peru), although there are at least four localities with records of *N. carceleni* south of the Amazon River (Hurtado & Pacheco 2017). *N. amoenus* in Northern Peru is limited to the north by the Marañon River, to the west by the Andes, and to the east by the Ucayali River. *N. amoenus* in Central Andes-Amazon is limited to the north by the Ucayali River and the foothills of the Andes. *N. spinosus* is limited to the north by the Andes (from the Choros valley to the Chiclayo valley in Peru), and the Huallaga River. Finally, *N. vargasllosai* is limited to the north by the Inambari River watershed in Puno Peru, to southern Bolivia in western Santa Cruz. These ranges seem to broadly agree with the Riverine Barrier Hypothesis (Wallace 1849; Patton et al. 1994; Brito et al. 2020). This is an interesting pattern because the distributions of several other biological groups have rejected this hypothesis (e.g., Patton et al. 1994, 2000; Haffer 2008; Defler 2019).

The samples MECN 5339 and MECN 5340 (**Fig**. 1) from Northwestern Ecuador form a clade (BS=73, PP=0.97) with *N. tenuipes* from Cundinamarca, Colombia (BMNH 1899.10.3.34/KX792081). We found a genetic distance of 6% between the Colombian and Ecuadorian samples (note that the sample of *N. tenuipes* KX792081 consists only of 177 base pairs). Additionally, morphological examination of the samples MECN 5339-40 and QCAZ 808, 891, 18677 showed several characteristics that differ from Colombian *N. tenuipes* (Voss et al. 2001): ventral fur pale, distinctive white color on throat and supra anal region; tail slightly longer than head-body length and unicolored; supraorbital ridges slightly curved backward; nasolacrimal capsule small; incisive foramina short, wide, and with subrectangular outline; septum of incisive foramina much broader. In light of this evidence, we consider that the Ecuadorian populations referred to *N. tenuipes* require a thorough revision.

Border conflicts between Ecuador and Peru, together with the establishment of several military detachments, the lack of access roads, and a soil not apt for agriculture, favored the conservation of the Cordillera del Cóndor ecosystems until the end of the 90s. However, since the Peace Agreement in 1998, colonization and consequent expansion of the agricultural-livestock frontier advanced over these areas. Thus, some research groups interested in studying biodiversity took advantage of the opening of the roads to carry out expeditions to such scarcely-known locations. These approaches have retrieved several descriptions of new species such as *Caenolestes condorensis*, *C. sangay*, *Rhipidomys albujai*, and *Thomasomys salazari* (Albuja & Patterson 1996; Ojala-Barbour et al. 2013; Brito et al. 2017, 2019). However, extensive mining operations have recently conducted (Roy et al. 2018), and access roads have penetrated numerous pristine areas of the mountain range (e.g., micro-basins of the Quimi, Machinaza and Nangaritza rivers), threatening one of Ecuador's regions of high diversity and endemism (Neill 2005; Almendáriz et al. 2014; Reyes-Puig et al. 2017). This highlights the urgency to decrease mining concessions in the Cordillera del Cóndor and establish comprehensive programs of biological inventory and collections, as well as to improve the access of scholars to these resources.

ACKNOWLEDGMENTS

It is an honor for us to contribute to this memorial volume to highlight the trajectory and work of Elio Massoia, an eminent mammalogist deeply involved in the study of Neotropical mammals. In this sense, we are grateful to the editors of the series of contributions, U. Pardiñas and C. Galliari for the opportunity to generate this tribute. We thank the company Kinross who hired the technical services of MEPN researchers to conduct faunal studies in several localities of the Alto Machinaza, through the consulting services of Entrix Inc. To N. Angamarca for his support during the field expeditions. N. Hurtado kindly provided us with morphometric data of *N. spinosus*, and photographs of various *Neacomys* species, including the holotypes of *N. amoenus* and *N. carceleni*. We thank V. Crespo-Pérez for reading the manuscript and M. Vega for making the map. JB and CK research is supported by the "Programa de cooperación Trilateral Alemania-Brasil-Ecuador", financed by the international cooperation GIZ. The laboratory work was funded by grants from Secretaría de Educación Superior, Ciencia, Tecnología e Innovación (SENESCYT, Arca de Noé Initiative; S. R. Ron and O. Torres-Carvajal as Principal Investigators). To the Dirección Provincial del Ministerio de Ambiente de Zamora Chinchipe for facilitating the research permits for this study N° 026-IC-FAU-DBAPVS-DRLZCH-MA and N°. MAE-DNB-CM-2016-0042 for access to genes.

LITERATURE CITED

Albuja, L., & B. D. Patterson. 1996. A new species of northern shrew-opossum (Paucituberculata: Caenolestidae) from the Cordillera del Cóndor, Ecuador. Journal of Mammalogy 77:41–53. https://doi.org/10.2307/1382707

Albuja, L., A. Almendáriz, R. Barriga, D. Montalvo, F. Cáceres, & J. L. Román. 2012. Fauna de vertebrados del Ecuador. Escuela Politécnica Nacional. Quito, Ecuador.

Almendáriz, A., J. E. Simmons, J. Brito, & J. Vaca-Guerrero. 2014. Overview of the herpetofauna of the unexplored Cordillera del Cóndor of Ecuador. Amphibian & Reptile Conservation 8:45–64.

ARCOM. 2015. Catastro minero del Ecuador. <http://geo.controlminero.gob.ec:1026/geo_visor>

Bradley, R. D., & R. J. Baker. 2001. A test of the genetic species concept: cytochrome-b sequences and mammals. Journal of Mammalogy 82:960–973. https://doi.org/10.1644/1545-1542(2001)082<0960:ATOTGS>2.0.CO;2

Berry, P. E., O. Huber, & B. K. Holst. 1995. Floristic analysis and phytogeography. In: Berry, P.E., Holst, B. & Yatskievych, K. (Eds.). Flora of the Venezuelan Guayana. St. Louis, Missouri Botanical Garden Press, pp, 161–191.

Brito, J., & A. Almendáriz. 2018. Una especie nueva de rana *Pristimantis* (Amphibia: Strabomantidae) de ojos rojos de la Cordillera de Cóndor, Ecuador. Cuadernos de Herpetología 32:31–40.

Brito, J., N. Tinoco, D. Chávez, P. Moreno-Cárdenas, D. Batallas, & R. Ojala-Barbour. 2017. New species of arboreal rat of the genus *Rhipidomys* (Cricetidae, Sigmodontinae) from Sangay National Park, Ecuador. Neotropical Biodiversity 3:65–79. https://doi.org/10.1080/23766808.2017.1292755

Brito, J., N. Tinoco, J. Curay, R. Vargas, C. Reyes-Puig, V. Romero, & U .f. J Pardiñas. 2019. Diversidad insospechada en los Andes de Ecuador: filogenia del grupo "cinereus" de *Thomasomys* y descripción de una nueva especie (Rodentia, Cricetidae). Mastozoología Neotropical 26:1–22. https://doi.org/10.31687/saremMN.19.26.2.0.04

Brito, J., C. Koch, A. R, Percequillo, N. Tinoco, M. Weksler, C. M. Pinto, & U. F. J. Pardiñas. 2020. A new genus of oryzomyine

rodents (Cricetidae, Sigmodontinae) with three new species from montane cloud forests, western Andean cordillera of Colombia and Ecuador. PeerJ 8:e10247. https://doi.org/10.7717/peerj.10247

Britz, R., A. Hundsdörfer, & U. Fritz. 2020. Funding, training, permits—the three big challenges of taxonomy. Megataxa 1:49–52. https://doi.org/10.11646/megataxa.1.1.10

Carleton, M. D., & G. G. Musser. 1989. Systematics studies of Oryzomyine rodents (Muridae, Sigmodontinae): A synopsis of *Microryzomys*. Bulletin of the American Museum of Natural History 191:1–83.

Carleton, M. D. 1973. A survey of gross stomach morphology in New World Cricetinae (Rodentia, Muroidea), with comments on functional interpretations. Miscellaneous Publications, Museum of Zoology, University of Michigan 146:1–43.

Clavel, J., G. Merceron, & G. Escarguel. 2014. Missing data estimation in morphometrics: how much is too much?. Systematic Biology 63:203–218. https://doi.org/10.1093/sysbio/syt100

Costa, B. M. A., L. Geise, L. G. Pereira, & L. P. Costa. 2011. Phylogeography of *Rhipidomys* (Rodentia: Cricetidae: Sigmodontinae) and description of two new species from southeastern Brazil. Journal of Mammalogy 92:945–962. https://doi.org/10.1644/10-MAMM-A-249.1

De Queiroz, K. 2005. A unified concept of species and its consequences for the future of taxonomy. Proceedings of the California Academy of Sciences 56:196–215.

De Queiroz, K. 2007. Species concepts and species delimitation. Systematic Biology 56:879–886. https://doi.org/10.1080/10635150701701083

Defler, T. 2019. The genesis of the modern Amazon River basin and Andean uplift and their roles in Mammalian diversification. In: History of Terrestrial Mammals in South America. Topics in Geobiology, vol 42. Springer, Cham. https://doi.org/10.1007/978-3-319-98449-0_12

Dowler, R. C., S. C. Darin, & C. W. Edwards. 2000. Rediscovery of rodents (genus *Nesoryzomys*) considered extinct in the Galapágos Islands. Oryx 34:109–118. https://doi.org/10.1046/j.1365-3008.2000.00104.x

Dupérré, N. 2020. Old and new challenges in taxonomy: what are taxonomists up against?. Megataxa 1:59–62. https://doi.org/10.11646/megataxa.1.1.12

Freile, J., et al. 2014. Birds, Nangaritza River Valley, Zamora Chinchipe Province, southeast Ecuador: Update and revisión. Check List 10:54–71. https://doi.org/10.15560/10.1.54

Granjon, L. 2005. Morphological and morphometrical analyses of three cryptic species of *Tatera* Lataste, 1882 (Rodentia: Muridae) from West Africa. Belgian Journal of Zoology 135:97–102.

Guayasamin, J. M., & E. Bonaccorso. 2011. Evaluación Ecológica Rápida de la Biodiversidad de los Tepuyes de la Cuenca Alta del Río Nangaritza, Cordillera del Cóndor, Ecuador. In: Guayasamin, J. M., & E. Bonaccorso. (Eds.). RAP Boletín de Evaluación Ecológica Rápida 58. Quito, Conservación Internacional.

Haffer, J. 1969. Speciation in Amazonian forest birds. Science 165:131–137.

Haffer, J. 2008. Hypotheses to explain the origin of species in Amazonia. Brazilian Journal of Biology 68:917–947. https://doi.org/10.1590/S1519-69842008000500003

Hershkovitz, P. 1940. A new spiny mouse of the genus *Neacomys* from Eastern Ecuador. Occasional Papers of the Museum of Zoology of University of Michigan 419:1–4.

Honaker, J., G. King, & M. Blackwell. 2011. Amelia II: a program for missing data. Journal of Statistical Software 45:1–47.

Hurtado, N., & V. Pacheco. 2017. Revision of *Neacomys spinosus* (Thomas, 1882) (Rodentia: Cricetidae) with emphasis on Peruvian populations and the description of a new species. Zootaxa 4242:401–440. https://doi.org/10.11646/zootaxa.4242.3

Jadán, O., & Z. Aguirre. 2011. Pp. 39–40, In: Evaluación Ecológica Rápida de la Biodiversidad de los Tepuyes de la Cuenca Alta del Río Nangaritza, Cordillera del Cóndor, Ecuador (Guayasamin, J. & E. Bonaccorso, eds.). Conservación Internacional, Quito, Ecuador.

Iucn. 2012. Categorías y Criterios de la Lista Roja de la UICN: Versión 3.1. Segunda edición. Gland, Suiza y Cambridge, Reino Unido: UICN. vi + 34pp. Originalmente publicado como IUCN Red List Categories and Criteria: Version 3.1. Second edition. (Gland, Switzerland and Cambridge, UK: IUCN, 2012).

Koutecky´, P. 2015. MorphoTools: a set of R functions for morphometric analysis. Plant Systematics and Evolution 301:1115–1121. https://doi.org/10.1007/s00606-014-1153-2

Kumar, S., G. Stecher, M.li, C.knyaz, & K.tamura. 2018. MEGA X: Molecular Evolutionary Genetics Analysis across computing platforms. Molecular Biology and Evolution 35:1547–1549. https://doi.org/10.1093/molbev/msy096

Lanfear, R., P. B. Frandsen, A. M. Wright, T. Senfeld, & B. Calcott. 2017. PartitionFinder 2: new methods for selecting partitioned models of evolution for molecular and morphological phylogenetic analyses. Molecular Biology and Evolution 34:772–773. https://doi.org/10.1093/molbev/msw260

Lessa, E. P., J. A. Cook, & J. L. Patton. 2003. Genetic footprints of demographic expansion in North America, but not Amazonia, during the Late Quaternary. Proceedings of the National Academy of Sciences 100:10331–10334. https://doi.org/10.1073/pnas.1730921100

Losos, J. B. 2008. Phylogenetic niche conservatism, phylogenetic signal and the relationship between phylogenetic relatedness and ecological similarity among species. Ecology Letters 11:995–1003. https://doi.org/10.1111/j.1461-0248.2008.01229.x

Mena, J. L., M. Williams, C. Gazzolo, & F. Montero. 2007. Estado de conservación de *Melanomys zunigae* (Sanborn 1949) y de los mamíferos pequeños en las Lomas de Lima. Revista Peruana de Biología 14:201–207.

Ministerio Del Ambiente del Ecuador. 2013. Sistema de Clasificación de los Ecosistemas del Ecuador Continental. Subsecretaría de Patrimonio Natural. Quito.

Neill, D. A. 2005. Cordillera del condor: botanical treasures between the Andes and the Amazon. Plant Talk 41:17–21.

Ojala-Barbour, R., C. M. Pinto, J. Brito, V. L. Albuja, T. E. Lee Jr & B. D. Patterson. 2013. A new species of shrew-opossum (Paucituberculata: Caenolestidae) with a phylogeny of extant caenolestids. Journal of Mammalogy 94:967–982. https://doi.org/10.1644/13-MAMM-A-018.1

Padial, J. M., A. Miralles, I. De La Riva, & M. Vences. 2010. The integrative future of taxonomy. Frontiers in Zoology 7:1–14. https://doi.org/10.1186/1742-9994-7-16

Pardiñas, U. F.J., et al. 2017. Cricetidae (true hamsters, voles, lemmings and new world rats and mice) - Species accounts of Cricetidae. In: Wilson, D.E., T. E. Lacher Jr, & R. A. Mittermeier, (Eds.), Handbook of the Mammals of the World. Rodents II v. Lynx Edicions, Barcelona pp. 280–535.

Pardiñas, U. F., C. Cañón, C. A. Galliari, J. Brito, Bernal N. Hoverud, G. Lessa, & J. A. De Oliveira. 2020. Gross stomach morphology in akodontine rodents (Cricetidae: Sigmodontinae: Akodontini): a reappraisal of its significance in a phylogenetic context. Journal of Mammalogy 101:835–857. https://doi.org/10.1093/jmammal/gyaa023

Patton, J. L, M. N. F. Da Silva, & J. R. Malcolm. 1994. Gene genealogy and differentiation among arboreal spiny rats (Rodentia: Echimyidae) of the Amazon basin: a test of the riverine barrier hypothesis. Evolution 48:1314–1323. https://doi.org/10.1111/j.1558-5646.1994.tb05315.x

Patton, J. L, M. N. F. Da Silva, & J. R. Malcolm. 2000. Mammals of the rio Juruá and the evolutionary and ecological diversification of Amazonia. Bulletin of the American Museum of Natural History 244:1–306.

R Core Team. 2019. R: A language and environment for statistical computing. R Foundation for Statistical Computing, Vienna, Austria. <https://www.R-project.org/>

Reig, O. A. 1977. A proposed unified nomenclature for the enameled components of the molar teeth of the Cricetidae (Rodentia). Journal of Zoology, London, 181:227–241.

Reyes-Puig, C., A, Almendáriz, & O. Torres-Carvajal. 2017. Diversity, threat, and conservation of reptiles from continental Ecuador. Amphibian & Reptile Conservation 11:51–58.

Ron, S. R. 2000. Biogeographic area relationships of lowland Neotropical rainforest based on raw distributions of vertebrate groups. Biological Journal of the Linnean Society 71: 379–402. https://doi.org/10.1111/j.1095-8312.2000.tb01265.x

Ron, S. R., M. Caminer, A. Varela-Jaramillo, & D. Almeida-Reinoso. 2018. A new treefrog from Cordillera del Cóndor with comments on the biogeographic affinity between Cordillera del Cóndor and the Guianan Tepuis (Anura, Hylidae, *Hyloscirtus*). ZooKeys 809:97–124. https://doi.org/10.3897/zookeys.809.25207

Ronquist, F. et al. 2012. MrBayes 3.2: efficient Bayesian phylogenetic inference and model choice across a large model space. Systematic Biology 61:539–542. https://doi.org/10.1093/sysbio/sys029

Roy, B., A. M. Zorrilla, L. Endara, D. C. Thomas, R. Vandegrift, J. M. Rubenstein, & M. Read. 2018. New mining concessions could severely decrease biodiversity and ecosystem services in Ecuador. Tropical Conservation Science 11:1–20. https://doi.org/10.1177/1940082918780427

Sánchez-Vendizú, P., V. Pacheco, & D. Vivas-Ruiz. 2018. An Introduction to the systematics of small-bodied *Neacomys* (Rodentia: Cricetidae) from Peru with descriptions of two new species. American Museum Novitates 3913:1–38. https://doi.org/10.5962/bhl.title.156671

Schulenberg, T., & K. Awbrey. 1997. The Cordillera Del Condor Region of Ecuador and Perú: a biological assessment. Washington, DC. Conservation International. (Rapid Assessment Program Working Papers 7).

Semedo, T. B. F. et al. 2020. Systematics of Neotropical Spiny Mice, genus *Neacomys* Thomas, 1900 (Rodentia: Cricetidae), from Southeastern Amazonia, with descriptions of three new species. American Museum Novitates 3958:1.

Sikes, R. S., & The Animal Care And Use Committee Of The American Society Of Mammalogists. 2016. Guidelines of the American Society of Mammalogists for the use of wild mammals in research and education. Journal of Mammalogy 97:663–688. https://doi.org/10.1093/jmammal/gyw078

Smith, M. F., & J. L. Patton 1993. The diversification of South American murid rodents: evidence from mitochondrial DNA sequence data for the akodontine tribe. Biological Journal of the Linnean Society 50:149–177.

Stamatakis, A. 2014. RAxML version 8: a tool for phylogenetic analysis and post-analysis of large phylogenies. Bioinformatics 30:1312–1313. https://doi.org/10.1093/bioinformatics/btu033

Strauss, R. E., M. N. Atanassov, & J. A. De Oliveira. 2003. Evaluation of the principal-component and expectation-maximization methods for estimating missing data in morphometric studies. Journal of Vertebrate Paleontology 23:284–296. https://doi.org/10.1671/0272-4634(2003)023[0284:EOTPAE]2.0.CO;2

Sullivan, J., E. Arellano, & D. S. Rogers. 2000. Comparative phylogeography of Mesoamerican highland rodents: concerted versus independent response to past climatic fluctuations. The American Naturalist 155:755–768. https://doi.org/10.1086/303362

Tribe, C. J. 1996. The neotropical rodent genus *Rhipidomys* (Cricetidae: Sigmodontinae): a taxonomic revision. Phd Thesis, University College, London.

Valencia, J. H, M. R. Duenas, P. Szekely, D. Batallas, F. Pulluquitín, & S. Ron. 2017. A new species of direct-developing frog of the genus *Pristimantis* (Anura: Terrarana: Craugastoridae) from Cordillera del Cóndor, Ecuador, with comments on threats to the anuran fauna of the region. Zootaxa 4353:447–466. https://doi.org/10.11646/zootaxa.4353.3.3

Vieites, D. R., K. C. Wollenberg, F. Andreone, J. Köhler, F. Glaw, & M. Vences. 2009. Vast underestimation of Madagascar's biodiversity evidenced by an integrative amphibian inventory. Proceedings of the National Academy of Sciences 106:8267–8272. https://doi.org/10.1073/pnas.0810821106

Vorontsov, N. N. 1967. Evolution of the alimentary system myomorph rodents (in Russian). Nauka, Siberian Branch, Novosibirsk.

Voss, R. S. 1988. Systematics and ecology of ichthyomyine rodents (Muroidea): patterns of morphological evolution in a small adaptive radiation. Bulletin of the American Museum of Natural History 188:262–493.

Voss, R. S., L. P. Lunde, & N. B. Simmons. 2001. The mammals of Paracou, French Guiana: A Neotropical lowland rainforest fauna. Part 2. Nonvolant species. Bulletin of the American Museum of Natural History 263:1–236.

Wallace, A. R. 1849. On the monkeys of the Amazon. Proceedings of the Zoological Society of London 20:107–110.

Weksler, M., & C. R. Bonvicino. 2015. Genus *Neacomys* Thomas, 1900. In: Patton, J.L., U.F.J. Pardiñas, & G. D'Elía, (Eds.), Mammals of South America. Vol. 2. The University of Chicago Press, Chicago, pp. 361–369.

Wiens, J. J., & C. H. Graham. 2005. Niche conservatism: Integrating evolution, ecology, and conservation biology. Annual Review of Ecology, Evolution, and Systematics, 36:519–539. https://doi.org/10.1146/annurev.ecolsys.36.102803.095431

Wiens, J.J., Et. Al. 2010. Niche conservatism as an emerging principle in ecology and conservation biology. Ecology Letters 13:1310–1324. https://doi.org/10.1111/j.1461-0248.2010.01515.x

Yazbeck, G. M., R. L. Brandão, H. M. Cunha, & A. P. Paglia. 2011. Detection of two morphologically cryptic species from the cursor complex (*Akodon* spp; Rodentia, Cricetidae) by RAPD markers. Genetics and Molecular Research 10: 2881–2892.

APPENDIX 1

Studied specimens belong to the following mammal collections: BMNH, Natural History Museum, London, UK; IAvH-M, Instituto de Investigación de Recursos Biológicos Alexander von Humboldt, Bogotá, Colombia; MECN, Instituto Nacional de Biodiversidad, Quito, Ecuador; MEPN, Museo de la Escuela Politécnica Nacional, Quito, Ecuador; MUSM, Museo de Historia Natural de la Universidad Nacional Mayor de San Marcos, Lima, Peru; QCAZ, Museo Pontificia Universidad Católica del Ecuador, Quito, Ecuador; and UMMZ, Museum of Zoology University of Michgan, Ann Arbor, USA.

Neacomys auriventer sp. nov. (n=14): Ecuador, Zamora Chinchipe, Cordillera del Cóndor, Vía Canales: MECN 5420, 5423; Paquisha Alto: MEPN 12078–79; El Zarza: MEPN 12086–87; Las Peñas: MEPN 11846, 11854, 12081, 12306, 12312, 12314, 12585, 12557.

Neacomys amoenus (n=1): Brazil, Serra do Chapada, Holotype: BMNH 3.7.7.84 (Photographic material).

Neacomys carceleni (n=48): Ecuador, Morona Santiago, Danu, Parque Nacional Sangay: MECN 4206, 4141; Domono: MEPN 11471; Napo, Challuayacu: MEPN 5890–91; vía Hollín–Loreto: MEPN 5894–5904; Cascada San Rafael: MEPN 5910–12; Llunchi, Rio Napo: Holotype: UMMZ 80171 (Photographic material).Orellana, Huiruno: MEPN 5889; Guiyero: MEPN 10715, 10723, 10733; Puente de Dosel Chiru: QCAZ 8163; Pompeya: QCAZ 15805, 15813; Parque Nacional Yasuní: QCAZ 15807, 15815, 15817, 16124, 16126, 16404, 16506–08, 16413, 16422; Pastaza, Comunidad de Kurintza: QCAZ 10364; Parque Nacional Llanganates: QCAZ 15251, 15253–54;

Sucumbíos, Pacayacu: MECN 3126; Tarapoa: MEPN 5913; Zábalo: QCAZ 7013, 7249, 7251; Destacamento Patria: QCAZ 7182; Tungurahu, Río Negro: QCAZ 4614; Zamora Chinchipe, Tundayme: MECN 5106.

Neacomys rosalindae (n=25): Ecuador, Morona Santiago, Taisha: MECN 476, 468–69; Orellana, Pompeya Sur: MECN 776, 791, 793, 968, 994, 1006; Comunidad Jabalí: MECN 2333; Pastaza, Lorocachi: MEPN 12363, 12371–72, 12387; Bameno: MEPN 12433, 12468, 12470–71, 12474–78; Zamora Chinchipe, Tundayme: MECN 5689–90.

Neacomys spinosus (n=1): Peru, Amazonas, Chachapoyas, Huampo, Lectotype: BMNH 81.9.7.25 (Photographic material).

Neacomys tenuipes (n=16): Ecuador, Carchi, Peñas Blancas: MECN 5340, 5370, 5372–76; Vía San Juan: MECN 2965; Esmeraldas, Río San Francisco: MECN 3058; Imbabura, Cielo Verde: MEPN 11720–21, 11728–29. Colombia, Antioquia, 25 km south and 22 km west of Zaragoza (La Tirana): IAvH-M-02935, 02938, 02980.

Neacomys vargasllosai (n=1): Peru, Puno, Sandia, Yanahuaya, Holotype: MUSM 35069 (Photographic material).

ONLINE SUPPLEMENTARY MATERIAL

Supplement 1

Table S1. Measurements of the *Neacomys* species used in the morphometric analysis (in mm): condylo-incisive length (CIL), zygomatic breadth (ZB); braincase breadth (BB), least interorbital breadth (IOC), length of rostrum (RL), length of the nasal bones (NL), breadth of rostrum (RW-1), orbital fossa length (OI), length of upper diastema (DL), crown length of maxillary toothrow (MTRL); length of incisive foramen (IFL); mastoid breadth (MB), basioccipital length (BOL); mesopterygoid fossa width (MPFW), breadth of zygomatic plate (ZPL), cranial depth (CP). Missing data are represented by na.

Table S2. List of specimens included in the phylogenetic analyses. For each terminal species, museum catalog numbers and GenBank accession numbers are provided. * Specimens' collector numbers, without museum numbers available; # Specimens used as outgroups.

Table S3. Gazetteer for *Neacomys auriventer* sp. nov., *N. carceleni*, *N. tenuipes* and *N. rosalindae*. Locality number according to **Fig**. 9.

Fig. S1. Phylogenetic tree resulting from Maximum Likelihood analysis. The red dashed line indicates the differences found in the phylogenetic relationships of certain species compared to the tree resulting from the Bayesian Inference analysis.

Fig. S2. Dorsal (A), lateral (B) and ventral (C) view of *Neacomys* species that inhabit eastern Ecuador. *Neacomys auriventer* sp. nov, (MEPN 12081) above; *N. rosalindae* (MECN 5824) center and *N. carceleni* (MECN 5865) below.